Team Carbonair Design Report

SAE — Super Mileage Vehicle

June 2011 Design Competition

Milwaukee School of Engineering

Written By:

Team Carbonair

Edited By:

Paul Gessler
Nerissa Hanson

Submitted:

May 23, 2011

Table of Contents

1 Advisor Approval **2**
2 Introduction **2**
3 Basic Vehicle Configuration **2**
4 Engine **3**
4.1 Fuel Injection 4
4.2 Fuel System 4
4.3 Variable Timing Ignition 4
4.4 Engine Displacement Reduction 5
4.5 Overhead Cam Conversion 5
5 Powertrain Configuration **6**
5.1 Clutch 6
5.2 Drivetrain 6
5.3 Engine Mount 7
6 Brake System **7**
6.1 Brake Selection 7
6.2 Caliper Mounting 8
6.3 Driver Control 8
7 Suspension and Running Gear **8**
7.1 Front Wheels 9
7.2 Rear Wheel 9
7.3 Suspension 9
7.4 Integrated Axle-Kingpin 11
7.5 Steering Linkage 11
7.6 Driver Controls 12
8 Chassis **13**
8.1 Core Material Selection 13
8.2 Carbon Fiber Analysis 14
8.3 Roll Bar 14
8.4 Rear Wheel Bracket 14
9 Body/Aerodynamic Shell **15**
9.1 Design Development 16
9.2 Accessibility 17
9.3 Construction Materials 17
10 Electrical System **17**
10.1 Existing Design 17
10.2 Power Management System 18
10.3 Data Acquisition System 19
11 Vehicle Performance **22**
12 Cost Estimate and Manufacturing Methods **23**
13 Driver Safety Features **24**
13.1 Guards/Body 24
13.2 Roll Bar 24
13.3 Firewall 24
13.4 Fire Extinguisher 24
13.5 Suspension 24
13.6 Mirrors/Visibility 25
Appendices **26**
A Detailed Expense Data **26**
B Engine Displacement Calculations **30**
C Intake Design **35**
D Dynamometer Tuning Equipment / Process **36**
E Complete Team Roster **37**

1 Advisor Approval

As Faculty Advisor for the Milwaukee School of Engineering SAE SuperMileage Team Carbonair, I have read and approved this report.

Advisor Name: _____

Advisor Signature: _____ Date:_____

2 Introduction

Returning for another year of competition, the Milwaukee School of Engineering (MSOE) Team Carbonair has designed and constructed an entirely new vehicle for competition in June 2011. The team, containing many returning members, concentrated on producing a more competitive vehicle in all aspects. The new platform features enclosed wheels to reduce aerodynamic drag, considerable weight reduction in the steering and chassis systems, powerful improvements to the electrical and data acquisition systems, and a heavily modified engine to reduce displacement and improve efficiency.

Constructing an entirely new vehicle is a major undertaking from a budget standpoint. Knowing this, the team made strong efforts to secure sponsorship for the new car. We maintained most of our past sponsors, while adding new sponsors to cover many major-cost items, including wheels, brakes, carbon fiber, electronic equipment, windshield molding, and foam core materials. MSOE has also been supportive of the project effort, providing work spaces, machine shop access, safety equipment, and opportunities to showcase our project to the school community. Team Carbonair is indebted to its sponsors and MSOE; the new vehicle simply would not be feasible without their continuing support.

This process of securing sponsors took place during the summer, after the June 2010 competition. Initial design work began during the summer as well. At the beginning of the academic year, the focus shifted to recruiting underclassmen for the team. This design team was founded at MSOE to encourage large design projects for underclassmen, well before they reach senior design. This approach gives vital early experience in engineering design, project management, and real-world group work. Through a series of events and open houses, there was an overwhelming response of interest in the team. Team Carbonair 2011 has over 30 members, all seeking a common goal: produce a single seat prototype vehicle to obtain the highest fuel mileage possible, all while complying with the official 2011 SAE SuperMileage Rules and following sound engineering practices. The combination of this goal and requirements will result in a high efficiency vehicle which is safe for the driver, team members, and spectators.

The construction of the vehicle is well underway. A rolling test chassis was assembled in February to test the handling and braking capabilities of the vehicle. The engine is now mounted to the test chassis to perform initial road testing. At the same time, the final composite chassis frame and body panels are being constructed. Once the initial testing is complete, all vehicle components will be transferred to the final chassis with body panels. The complete vehicle will be finished by May, allowing for a full month of final testing to resolve any unforeseen problems and perform final tuning of the components.

This report documents the design of MSOE's Team Carbonair 2011 SuperMileage vehicle. It presents the focus and goals of the team, and explains design/manufacturing decisions while also illustrating official 2011 SAE SuperMileage Rules compliance.

3 Basic Vehicle Configuration

The 2011 MSOE SuperMileage Vehicle (SMV) is a single-seat, three-wheeled, gasoline-powered vehicle designed to compete in the SAE SuperMileage Competition. The main structure of the vehicle is formed by two composite frame rails running the length of the vehicle. These frame rails are of carbon fiber-vinylester resin construction, with a rigid foam core material. The mid-mounted Briggs and Stratton engine (Model 091202), sleeved to displace 50 cc and utilizing an overhead cam, drives the single 20 in rear wheel via a chain drive with a 1:5.65 gear ratio. The two 20 in front wheels steer

the vehicle and are connected to the driver controls via adjustable mechanical linkages. The vehicle configuration is shown in Fig. 1.

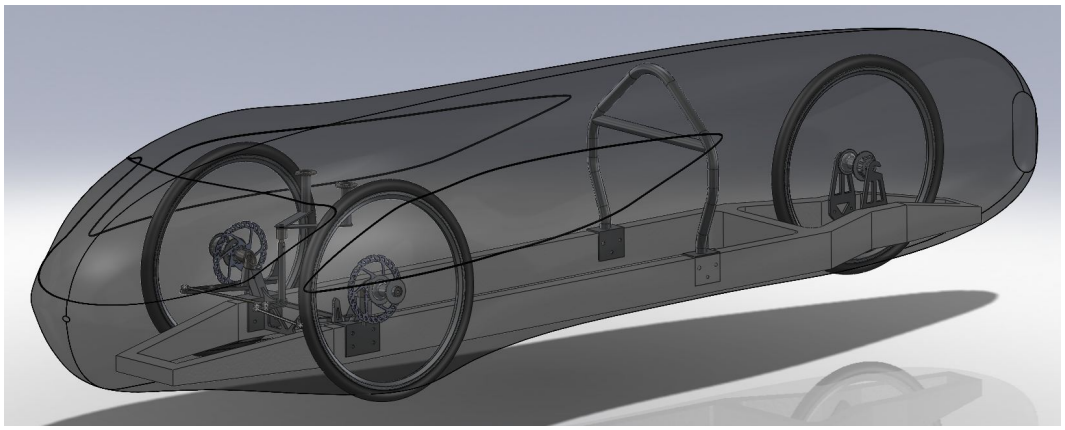

Figure 1: Basic Vehicle Configuration

The driver controls the vehicle from a reclined position, with his/her feet facing the direction of travel. A five point harness is employed to restrain the driver in the event of a collision or failure. All driver controls are attached to a steering wheel for ease of operation. The vehicle body is a carbon fiber-vinylester resin composite with large polycarbonate windshields for visibility. Access to the interior of the vehicle is provided by one large hatch forward of the firewall/roll bar (for driver entry/exit) and several hatches behind the firewall to access mechanical and electronic equipment.

The overall vehicle dimensions are 115 in long, 35 in wide, and 24 in high. The ride height of the vehicle is 3 in. The SMV has a wheelbase of 66 in and a front track width of 24 in. The wheelbase was selected based on the space required for all components and a driver placement which gave a stable center of gravity location. The rear wheel axle centerline is located 12.85 in forward of the aft edge of the frame rails, which are 98 in long overall. The body extends 8.3 in beyond the front edge of the frame rails. The roll bar reaches a total height of 23 in and is mounted 24.5 in forward of the rear wheel axle.

4 Engine

The engine is one of the most crucial components to achieving high fuel efficiency because this is where the fuel's energy is directly utilized when it gets converted from chemical energy to mechanical energy. Therefore, this part of the car needs to be well researched, well built, and well tested. The main purpose of the engine is to convert the smallest amount of fuel to mechanical energy in order to complete the task at hand. In this case, it will be powering a single occupant vehicle of approximately 220 total pounds around a 1.6 mile track 6 times. To achieve this, the team completed a series of calculations (see Appendix B) to determine just how much power is required from the engine. This information provided the basis for the power output required from the engine to efficiently propel the car around the track.

The base engine regulated by SAE for this competition is a 3.5 hp Briggs and Stratton Model 091202 Type 1016E1A1001. Compared to the power output required, this engine is approximately three times too powerful. This engine uses a flat head or L-head design, which is a design that has been used extensively since internal combustion engines have become popular. This design, however, has been phased out as increasingly efficient engine configurations have come into favor. The problem with the L-head engine is that it has a low compression ratio of about 6:1, and the combustion chamber is not directly over the piston but instead over the intake and exhaust valves which are in a parallel configuration with the piston. The Briggs and Stratton engine also has a fixed ignition timing system that is set to run at a fairly retarded timing. This allows the engine to run at all the operating RPMs but does not allow for optimum efficiency. Retarded timing limits in-cylinder pressures and temperatures and leads to lower efficiency. Advancing the timing allows higher pressures during the beginning of the power stroke resulting in higher power and efficiency.

For the reasons stated above, the team has decided to modify the engine in the following ways: add electronic fuel injection, add a variable timing ignition system, reduce the engine displacement to 50cc, and convert from L-head to overhead cam configuration. These four modifications are all allowable in the official 2011 SAE Supermileage Rules and will be properly monitored to ensure safe operation. A detailed list of engine parts can be found in Appendix A.

4.1 Fuel Injection

This year's engine will employ the same electronic fuel injection (EFI) system utilized on the 2009–2010 MSOE SuperMileage Vehicle, using a Bosch Model 0280155989 injector. This system uses an Electronic Control Unit (ECU) donated by Control Systems, Inc., Model FCR-5. The system includes many sensors to monitor the engine including block temperature, ambient air temperature, crank position, oxygen concentration in the exhaust, and throttle position. These sensors have been chosen to monitor the system based on the fact that the engine has a single cylinder. Most standard automobiles utilize the first 4 sensors listed and a built-in algorithm to adjust the injection volume from a base map. The reason a throttle position sensor (TPS) was chosen over a mass air fuel (MAF) or a mass air pressure (MAP) sensor is because of large fluctuations in the readings from the latter two sensors when tested in the intake manifold. The TPS provides a more stable reading for the EFI by monitoring the angle of the throttle plate. This is not the optimum way to monitor the amount of air entering the system, but the stable reading will provide ample accuracy for this application, without the fluctuations that MAF or MAP sensors induce. With this and the new dynamometer setup for tuning the engine, described in Appendix D, the fuel map created within the ECU will be tuned for optimum efficiency throughout the entire RPM and throttle angle ranges.

4.2 Fuel System

The fuel pump used is a Neuberger, Inc. Model NF30KP.27DC. This pump was chosen because it has the correct flow rate, 0.3 L/min, and pressure, 45 psi, needed to operate the fuel injector.

The fuel regulator in this fuel system is a Megan Racing fuel pressure regulator. This regulator was chosen because it is in the price range of the team budget and it meets all the required specifications for the fuel system. These specifications are that it must *a*) set and maintain a user-defined fuel pressure, *b*) operate between 0-50 psi, *c*) have a fuel pressure gage, and *d*) work with a return-type fuel system. Figure 2 is a diagram of the fuel system, showing the location of all components, including all valves and tees used to connect these components. All fuel hoses are Tygon F-4040-A 1/8IDx1/4OD. This hose has a maximum working pressure of 50 psi and all connections are secured with wire hose clamps. Note that when V-1 is open and V-2 is closed, the system is operating on carburetion. When V-1 is closed and V-2 is open, the system is operating on electronic fuel injection. The carburetion option allows early testing with the stock configuration until the EFI system is fully completed. The item in Fig. 2 labeled 'Pressure Relief Valve' also serves as the dump valve to depressurize the system for fuel bottle replacement. The fuel bottle is mounted to the back of the firewall with an aluminum bracket and rubber strap, allowing easy access through the rear hatch. Any leaked fluids from the engine area drain into a well and out of the body as described in Section 8.

4.3 Variable Timing Ignition

The timing on the stock Briggs and Stratton Engine is not adjustable, and by leaving the ignition in a fixed state, peak efficiency cannot be attained. Since the engine is not running at a constant RPM when in use, the ignition pack timing cannot be set to a single RPM setting and left there for the duration of the engine's life without compromising efficiency. For this reason, variable timing ignition has been added to the stock engine. This ignition system receives its power from the flywheel by charging the ignition packs using magnets in the flywheel. Instead of sending this power directly to the engine to create the spark at the fixed timing, the power will be directed into the ECU. This ECU has the capability to temporarily hold the charge until the engine is in the correct position on the compression stroke to begin the ignition of the fuel. The flame from the spark plug needs time to propagate to the entire volume of the cylinder to properly ignite all of the fuel. The best efficiency is achieved when the most amount of fuel is being ignited near TDC, thus causing the highest pressure and the most

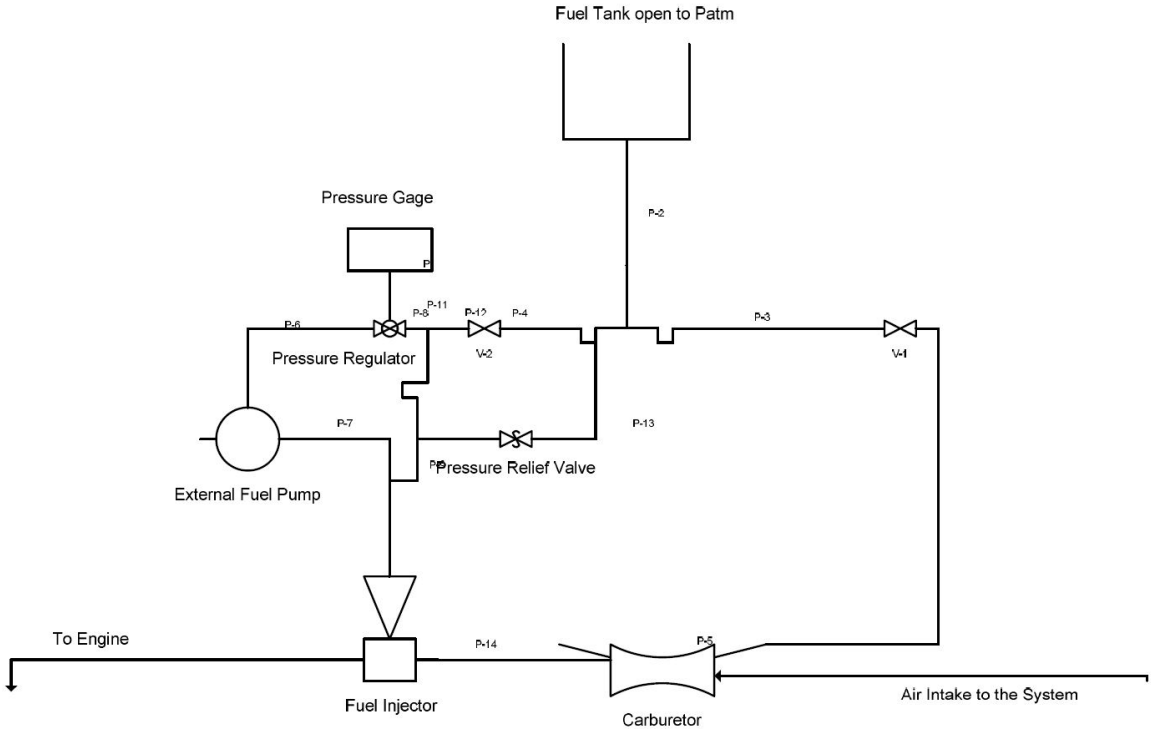

Figure 2: EFI Fuel System Diagram

work output on the down stroke. In this way, the timing can be retarded at low RPM and advanced at higher RPM to obtain optimum flame propagation. In order to achieve a working variable timing ignition system on the Briggs and Stratton engine, a donated Mercury Marine ignition system will be retrofitted. This is a custom system currently being developed by the team in conjunction with Mercury Marine and Control Systems, Inc.

4.4 Engine Displacement Reduction

With the current base engine having too much power output for the application, the team decided that reducing the engine displacement would also be beneficial in improving the fuel economy of the vehicle. To achieve this, a reducing cylinder called a sleeve will be added to the engine block, reducing the displacement from 148cc to 50cc. A new piston, the Wiseco XR-50 88-03 CRF-50F, is used in the sleeve, and a new connecting rod will be designed. This new displacement was determined through a series of calculations modeling the Otto Cycle for 4-stroke engines. These calculations are presented in Appendix B of this report. Through these calculations, the team was able to estimate the required power output of the engine and determine that the 50cc displacement will in fact produce enough power to effectively and efficiently move the vehicle under all load requirements of the competition. The scenarios modeled for the calculations used assumptions from the worst case scenario where the engine would require the most power. These included accelerating at a given rate up an incline typical to that found at the Eaton Proving Grounds. The final results of the calculations show that the SMV requires about 0.7 hp to start from 0 mph and accelerate to a speed of 30 mph at a rate of 1 mph/s while traveling up a 1° incline. The 50cc engine will provide an expected 0.9 hp.

4.5 Overhead Cam Conversion

The most drastic change to the engine will be the head conversion from the standard L-head to the overhead cam head. This is an extreme change from the original engine because instead of the valves residing in the block parallel to the cylinder, the intake and exhaust valves will now be located directly above the combustion chamber. An overhead configuration of the valves will allow a higher compression ratio and better volumetric efficiency. With a higher compression ratio, engine efficiency

also improves. A major challenge with this type of configuration is timing the camshaft with the crankshaft to ensure proper cycling of the engine. If this is not done properly there is a chance that the valves could possibly run into the piston as it is moving up in the cylinder. Also, the possibility of backfire through the intake port is increased. Without proper alignment between shafts, the engine will not run properly or work anywhere near as efficiently as expected. A custom chain drive is being planned to time the camshaft. With the new head configuration, the intake manifold has been redesigned to use the EFI system to optimize fuel consumption, using a bell-mouth entrance (loss coefficient $K_l = 0.04$) into an integrated part which houses the injector, throttle body, throttle limit screws, and TPS. The new intake design is shown in Fig. 27 in Appendix C. A new exhaust manifold is being designed to direct the exhaust out of the vehicle body with as few losses as possible. The engine orientation allows the insulated exhaust pipe to exit nearly straight out the back of the vehicle, protruding one inch beyond the body panels. This manifold will also house the oxygen sensor.

The conversion to overhead cam is the most difficult to complete but is also the most beneficial when combined with the reduced engine displacement.

5 Powertrain Configuration

The powertrain of the SMV must transmit power from the engine to the rear drive wheel in the most efficient, safe, and reliable manner possible. A fixed gear ratio was chosen based on the narrow range of speeds at which the vehicle is required to operate. As with last year's vehicle, a chain drive was selected for its high efficiency, great wear resistance, and exceptional reliability.

5.1 Clutch

A Horstman X5-D1 single-disc centrifugal clutch, purchased directly from the manufacturer, is installed on the car. A clutch is needed to keep the car stationary while at idle. A centrifugal clutch was selected over a manual clutch for ease of installation and operation. The stall speed of the clutch is approximately 2100 rpm, allowing disengagement while the vehicle is idling.

5.2 Drivetrain

A chain drive system is used to transmit power because of superior reliability and efficiency compared to a belt drive. A sprocket prevents the chain from slipping, which ensures that the engine's power is not wasted. A #219 racing cart chain was selected instead of a standard #35 chain to transmit the power from the sprocket on the clutch of the engine to the sprocket attached to the rear wheel. The #219 chain used weighs 0.206 lbf/ft, which is lighter than any #35 chain. It also has a 18.4% smaller pitch, resulting in more contact points per inch and smoother operation. A steel 17 tooth #219 sprocket was used on the clutch, and a 6061 T6 aluminum 96 tooth sprocket was placed on the rear wheel to produce a 1:5.65 gear ratio, resulting in a vehicle top speed of approximately 40 mph at 3600 rpm, as shown in Eq. 1:

$$v = N_e M_v = \left(3600\frac{\text{rev}}{\text{min}}\right)\left(\frac{1}{5.647}\right)\left(\frac{20\pi \text{ in}}{1 \text{ rev}}\right)\left(\frac{60 \text{ min}}{1 \text{ hr}}\right)\left(\frac{1 \text{ ft}}{12 \text{ in}}\right)\left(\frac{1 \text{ mi}}{5280 \text{ ft}}\right) = \boxed{37.9 \text{ mph}} \quad (1)$$

where N_e is the engine speed and M_v is the gear ratio.

A sprocket-hub adapter was designed in SolidWorks to mate the hub and the 96 tooth sprocket. The adapter was manufactured on a CNC mill from 6061-T6 Aluminum and is shown in Fig. 3. The 96 tooth sprocket bolts into the adapter, which is attached to the rear hub via epoxy.

Experimental testing showed that this epoxy can withstand a torque of 120 ft-lbf in this configuration, leading to a factor of safety of 37, as computed in Eqs. 2 and 3:

$$T_{\text{adapter}} = \frac{T_{\text{sprocket}} * r_{\text{adapter}}}{R_{\text{sprocket}}} = \frac{31 \text{ ft-lbf} * 0.5 \text{ in}}{4.7 \text{ in}} = 3.26 \text{ ft-lbf} \quad (2)$$

$$N = \frac{T_{\text{allowed}}}{T_{\text{applied}}} = \frac{120 \text{ ft-lbf}}{3.26 \text{ ft-lbf}} = \boxed{37} \quad (3)$$

Figure 3: Sprocket-Hub Adapter

5.3 Engine Mount

Two requirements were considered when designing the engine mount: weight and ease of adjustment. The engine will be permanently attached to L-shaped aluminum brackets on the bottom of the block, which are allowed to slide freely along the sides of a rectangular 80/20 aluminum rail as seen in Fig. 4. The L-shaped motor brackets can be tightened down with bolts to lock the engine in place. These bolts attach to the side of the rail, making them easy to access with a socket. This design can be seen in Fig. 5. To counteract the force of the chain and keep the engine stationary, an adjustable stop is bolted to the top of the 80/20 rail.

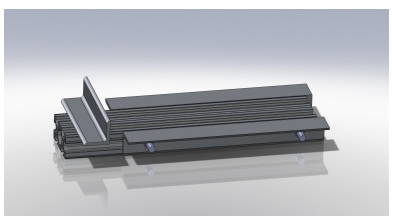

Figure 4: Engine Mount Design

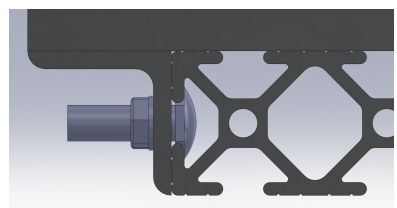

Figure 5: Carriage Bolt Design

The engine is mounted as close to the centerline of the vehicle as possible to improve weight distribution. The left-side drive hub allows for this, as discussed in Section 7.

6 Brake System

The objective of the brake system is to safely slow and/or stop the vehicle, keeping the driver, team members, and spectators safe. The requirements of the brake system are as follows: *a*) slow the vehicle to a stop from 15 mph within 13 ft, *b*) allow for easy driver control in any situation, and *c*) produce minimal drag when not in use to improve efficiency.

6.1 Brake Selection

HB Performance Systems, Inc. (HBPSI) was very generous in sponsoring the brake system. In working with them to select the components, all the above requirements were kept in mind. Many of HBPSI's brake products are designed for use on mountain bikes, which have similar if not greater braking demands than the SuperMileage vehicle. To confirm this, a basic kinetic energy comparison of the two vehicles is presented in Eqs. 4 and 5. For the SMV (Eq. 4), a combined vehicle and driver mass of 200 lbm is used (130 lbm driver, 70 lbm vehicle), and the vehicle is traveling at its maximum speed of 38 mph (from Eq. 1).

$$E_{\text{k,SMV}} = 0.5 * m_{\text{SMV}} * v_{\text{SMV}}^2 = 0.5 * 200 \text{ lbm} * (38 \text{ mph})^2 = 144400 \text{ lbm-mph}^2 * \frac{0.090648 \text{ J}}{\text{lbm-mph}^2} = 13.1 \text{ kJ} \tag{4}$$

For the mountain bike (MTB, Eq. 5), a combined vehicle and rider mass of 205 lbm is used (180 lbm rider, 25 lbm bike), and the bike is traveling at 40 mph, a speed commonly seen in downhill sections of mountain bike races.

$$E_{\text{k,MTB}} = 0.5 * m_{\text{MTB}} * v_{\text{MTB}}^2 = 0.5 * 205 \text{ lbm} * (40 \text{ mph})^2 = 164000 \text{ lbm-mph}^2 * \frac{0.090648 \text{ J}}{\text{lbm-mph}^2} = 14.9 \text{ kJ} \tag{5}$$

The results of this comparison show that a brake system from a racing mountain bike is more than adequate. In anticipation of needing brakes on all wheels for a different competition or rule changes, the brakes were selected to mount on the two front wheels (a rear brake can easily be added if required in the future). This necessitates a disc brake design, since there is no suitable mounting point for rim brakes around the periphery of the front wheels. Additionally, a hydraulic system was selected to eliminate any brake-pull issues that would arise from any cable system driving two brake calipers.

On all mountain bikes, each brake caliper has its own dedicated master cylinder and reservoir. The situation on the SMV is unique because one master cylinder/reservoir controls two calipers. Therefore, the components were carefully selected to ensure enough brake fluid capacity in the system. Two self-centering, small-bore, double-piston El Camino disc brake calipers were selected with 160 mm rotors, the same size commonly used on racing mountain bikes. A large-bore Stroker Trail master cylinder was selected to control the brakes. A small steel tee-junction was machined to allow each caliper to be in the same hydraulic circuit as the shared master cylinder. The combination of the two small-bore calipers and large-bore master cylinder provides a balanced system with normal brake lever travel.

Initial road testing using the test chassis has confirmed that the brake system meets the stopping distance requirement of 13 ft from 15 mph. The brake balance has been tested as well; the vehicle does not pull left or right under heavy braking. The system uses readily available DOT 4 brake fluid and uses industry-standard fittings and bleed kits, which will ease repairs and re-bleeding if necessary.

6.2 Caliper Mounting

The El Camino calipers were mounted directly to the output links of the steering control linkages. These links were designed to handle the substantial loading the calipers add under heavy braking. A detailed documentation of this design can be found in Section 7.

6.3 Driver Control

The brakes will be controlled by the driver using the Stroker Trail integrated master cylinder/lever described above. This lever will be mounted on the steering wheel (described in Section 7) to provide centralized control for the driver. This is critical because the driver needs access to all vehicle controls in any situation. Placing the brake lever on the steering wheel ensures that he/she will be able to slow or stop the car while steering at the same time.

7 Suspension and Running Gear

The purpose of the steering system is to support the vehicle during the dynamic events and provide a means for the driver to control the car. The SMV needs to turn within the required turning radius of 50 feet along with successfully navigating the slalom course. The steering must allow the driver to steer the car comfortably while maintaining access to the throttle and brake controls in all situations. The decision to use inboard front wheels necessitated a very compact design and close integration with the chassis frame rails.

The running gear of the vehicle (wheels, tubes, and tires) must provide adequate traction on the track surface as well as supporting the vehicle. The main objective in selecting running gear was minimizing rolling resistance and weight, while adhering to the 2011 SAE SuperMileage Rules and ensuring safety for all participants through sound engineering practices. As with the brake system, HBPSI sponsored the running gear components.

7.1 Front Wheels

Since the two front wheels are completely enclosed by the body shell, 20 in BMX wheels were selected. These wheels are compact and easily capable of withstanding loading during the dynamic events.

For the front wheels, disc hubs were needed for compatibility with the hydraulic disc brake system discussed in Section 6. Another unique requirement is the method of wheel support in the SMV. Unlike traditional BMX wheels whose axles are supported at both ends, the geometry of the steering package requires that the wheel is cantilevered, or supported on only one end of the axle. The only commercially available hub that satisfies these requirements is the Cannondale Lefty hub, which is prohibitively expensive and not readily available. A solution was found in the Sun-Ringlé Abbah Downhill 32H front hub. Manufactured by HBPSI, this hub uses the ISO Standard 6-bolt disc pattern shared by the brake rotors. Although not specifically designed for cantilever support, it uses a 20 mm thru-axle and is designed for the abuse of downhill racing. The thru-axle design combined with a steel axle and kingpin as discussed below ensures that these hubs can meet all requirements. Two Abbah DH front hubs were donated for use on the front wheels.

The front rims must be lightweight, designed for narrow, high-pressure 20 in tires, and have the same 32H spoke count as the Abbah DH hubs. After working with HBPSI to select a rim, the Sun-Ringlé Assault SL-1 was selected. These rims feature double-wall construction and sleeved spoke holes to reduce fatigue. The Assault SL-1 is designed for racing and thus is very lightweight and rated to 120 psi, which is ideal for the SMV. Two Assault SL-1 rims were donated for use on the front wheels. The rims are laced to hubs via double-butted alloy spokes, also donated by HBPSI. They follow a three-cross lacing pattern to handle any potential side loading and transfer torque to the disc brakes.

The front tires must offer a smooth tread surface and high pressure capability (>100 psi) to reduce rolling resistance. Primo Comet 20x1 1/8″ tires were selected since they have a very fine tread pattern and rated to 110 psi. Two of these tires were purchased from a local bike shop.

7.2 Rear Wheel

The rear wheel is also a 20 in BMX wheel since the same considerations apply. The rear wheel has the added requirement of being left-side drive for optimal engine placement.

A freecoaster rear BMX hub was chosen for the rear wheel for multiple reasons. A BMX hub was selected because it has the largest market for left-side drive hubs. A freecoaster hub was selected for its near-frictionless and silent rolling when the driving mechanism is not engaged. This differs from a standard cassette or freewheel hub where the driving mechanism (usually a series of racheting pawls) creates friction and noise, which wastes energy. The final hub chosen is the KHE Astern LHD 36H, purchased from a local bike shop. This hub was chosen for its unique adjustability of the freecoaster clutch mechanism.

The rear rim must deliver the engine torque to the track surface and supports most of the weight of the vehicle. Though weight considerations are paramount in any high mileage vehicle, this critical component was selected based on durability. A Sun-Ringlé Rhyno Lite XL 36H rim was selected and donated by HBPSI. This rim is laced to the KHE Astern rear hub in a three-cross pattern for maximum durability, and is shod with a 20x1.95″ KHE Mac 1.5 folding-bead tire, purchased from a local bike shop. This tire features a Kevlar bead, which is both stronger and lighter than a standard wire bead. The tire's maximum inflation rating of 120 psi and smooth tread pattern both serve to reduce rolling resistance.

7.3 Suspension

The suspension of the SMV is designed to be rigid to reduce drive and rolling losses. Any compliance and damping in the system is provided by the tires. To reduce spoke breakage issues encountered with last year's vehicle, Milliken and Milliken's 'Race Car Vehicle Dynamics' [8] was consulted. Even though the applications are quite different, many of the same techniques can be used to reduce wheel loading under demanding dynamic events. Caster was used to provide a righting moment in the controls such that the vehicle would return to straight-line travel without driver input. This eliminates weaving and makes driving the vehicle much easier. Camber was introduced to make the

steering package more compact while allowing ample room for the driver between the wheels. This combination of camber and caster has the added benefit of leaning the wheels into the turn, reducing side loading of the front wheels. An Excel spreadsheet was created to find the optimum caster and camber angles for a 66 in wheelbase and 24 in track width. Design parameters of 5° caster and 6° camber were selected for the suspension geometry.

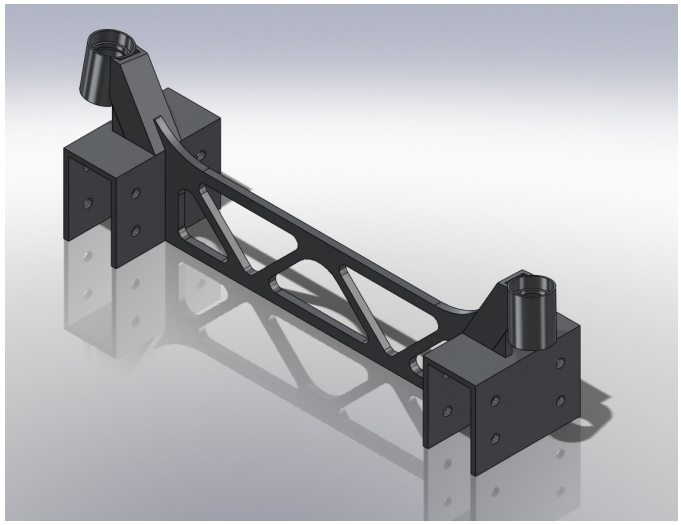

Figure 6: Suspension Frame Design

The suspension frame must provide the correct steering geometry. These requirements include the 24 in track width, 5° caster, and 6° camber. It also must provide the desired 3 in vehicle ride height. Given the restricted space between the axle centerlines and the top of the chassis frame rails, a semi-tubular suspension frame was designed and constructed of 6061-T6 Aluminum. The cross member fits between the frame rails; any other location would have either blocked visibility or restricted driver space. The frame design has c-channels which allow attachment to the composite frame rails via shoulder bolts. A bolt diameter of 5/16″ was selected through work with the chassis team. This size is relatively compact, yet large enough to distribute the load through the carbon fiber and foam core effectively. The steering frame design is presented in Fig. 6. The cross member supports the frame rails and helps transfer the load to the chassis, and is machined from 0.25 in plate with a CNC Waterjet. The time on this machine was graciously donated by TAK Engineering, Inc. The c-channels are combinations of commercial aluminum extrusions, and the square tube uprights are CNC machined on MSOE's HAAS Machining Center from 0.125 in wall, 1 in square tube. The kingpin tubes themselves are machined from 1.125 in tube in MSOE's machine shop.

A stress analysis of this design was conducted using SolidWorks Simulation. Load cases for side loading during turns and static loading were conducted, however, the limiting load case was the dynamic load simulation which represents severe bumps that may be encountered during testing. This load case consisted of a 1000 lbf load being applied to each kingpin bushing seat simultaneously; this is the equivalent of a 10G vertical deceleration of the vehicle. The stress analysis also took into account weakened areas near welds in the design. The results showed a minimum factor of safety of 1.8 in the area between the upright and the c-channel. This factor of safety is adequate for the suspension frame, since the dynamic load case is very conservative. The sizes of the kingpin tubes were defined by the design of the integrated axle-kingpin, as described below.

Strain gauges have been placed on the suspension in the critical areas. A single rosette gauge was placed in the critical area between the square tube upright and the c-channel and a single axial gauge was placed on the outer surface of the cross member. Using a Vishay Model P3 Strain Indicator, strain data has been logged during test sessions. These data are used to monitor the stresses created by bumps and rough roads to confirm that the dynamic loading case used for the design analysis is similar to the loading generated by actual road inputs. The Von Mises Effective Stress is calculated from the rosette strain readings and compared to the yield stress of 6061-T6 Aluminum to obtain the factor

of safety. So far, many combinations of sharp turns, heavy braking, and rough roads have produced a minimum factor of safety of 2.3, supporting the conclusion of a conservative dynamic load case.

7.4 Integrated Axle-Kingpin

As mentioned above, the front wheels are supported in a cantilevered fashion, preventing a traditional axle support. To reduce the number of components in the system, a single part will function as both the axle and kingpin for the steering system. Such a part needs high surface hardness since rolling bushings will be used in the kingpin tube. It also must be nearly rigid to maintain the desired steering geometry and provide responsive vehicle control. These considerations, along with ease of welding and thread-holding qualities, played a large role in the selection of steel for this component. The design of the integrated axle-kingpin is presented in Fig. 7.

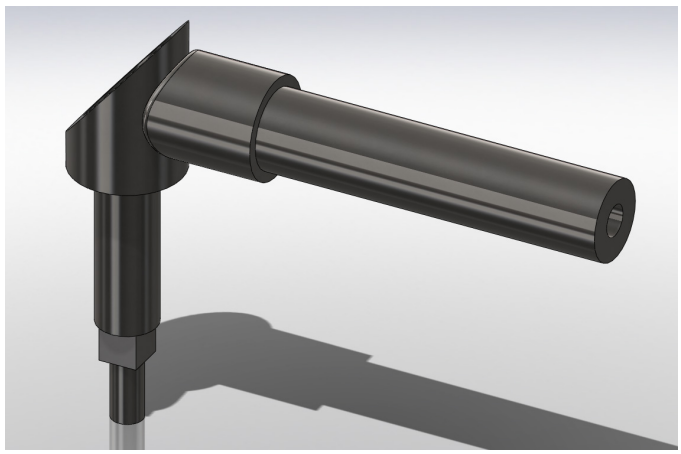

Figure 7: Integrated Axle-Kingpin Design

Both shafts are hollow to minimize weight. The axle is internally threaded to fasten the front wheel, while the kingpin has a square section to accept the output link of the steering linkage, with external threading for fixing bolts. The kingpin rotates on lower and upper bushings made of MDS-filled nylon. This nylon was chosen because of its excellent wear properties and low friction. These bushings transmit axial and transverse loading into the suspension frame. This part has a minimum factor of safety of 4.5 in the dynamic load case discussed above.

7.5 Steering Linkage

The steering linkage must convert driver input to kingpin rotation. To minimize drag forces, a nearly perfect Ackermann steering geometry is desired through the radii the SMV will see on the track (>50 ft). A series of Excel spreadsheets were created to compare several different linkage configurations, including a simple Pitman arm input, trapezoidal rack and pinion, and a Pitman triangle. The results of these comparisons show that the Pitman triangle approach provides the most compact solution which provides the correct Ackermann geometry. The final Pitman triangle is shown in Fig. 8, and is manufactured on MSOE's CNC Mill out of 6061-T6 Aluminum.

The coupler links to each front wheel are steel tie rods to provide adjustability in the system. The output links of the steering linkages also serve as the mounting points for the brake calipers. Therefore, the torque about the kingpin axis while turning and the substantial loading under heavy braking must be considered in analyzing these components. The links are made from 3/8" 6061-T6 Angle Aluminum for ease of manufacturing. They were manufactured on MSOE's CNC Mill. Note that the links are highly asymmetrical because the mountain bike brake calipers are designed to mount on one side of the bike. Since the wheel is only supported on the inboard side, one of the caliper/rotor combinations needs to face the opposite direction.

Figure 8: Pitman Triangle Design

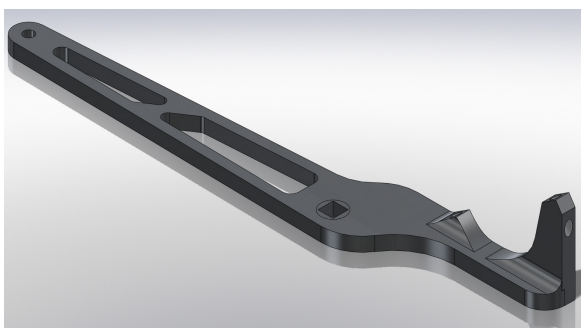

Figure 9: Left Side Output Link

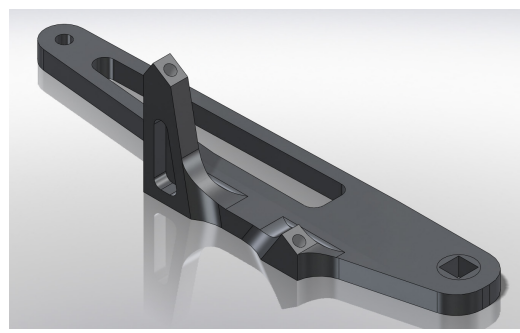

Figure 10: Right Side Output Link

The analysis of these links was done based on a number of load cases. The worst case scenario was found to be the combination of turning torque and maximum brake torque. The maximum force created by the turning torque is 90 lbf, computed using the measured maximum torque generated by the drivers in basic testing and the ratio of link lengths. The force generated under heavy braking was calculated for a case where the brakes are just about to lock up the front wheels, as in Eq. 6:

$$F_B = \frac{RF_f}{r} = \frac{RF_n\mu_s}{r} = \frac{(10.25 \text{ in})\,(70 \text{ lbf})\,(0.9)}{3.15 \text{ in}} = \boxed{205 \text{ lbf}} \tag{6}$$

where F_B is the brake mount force, R is the wheel radius, F_n is the weight supported by each wheel, r is the disc radius, and μ_s is the coefficient of static friction between the rubber tire and asphalt road surface. This force acts in the direction tangential to the brake mount plane. SolidWorks Simulation analysis of these load cases resulted in a minimum factor of safety of 2.4 for these parts.

The linkage allows for 18° of rotation for each wheel, more than enough for the requirements of the SMV. Based on the 66 in wheelbase and 35 in vehicle width, a turn angle of about 15° is required in the slalom course, about 12° is required for the 50 ft radius arc before the slalom course, and only about 9° of wheel movement is required on the Eaton Proving Grounds during the fuel mileage runs.

7.6 Driver Controls

The driver controls for the vehicle must allow for smooth, natural control of the steering, provide suitable mounting points for brake and throttle controls, and be movable to ensure easy entry/exit for the driver. Several design concepts were explored, including lever systems and cable/pulley systems, however, the best use of space was the steering wheel on an angled column. This design provides a central

mounting location for throttle, brake, and starter controls without reducing visibility or available space. The column can easily break away from its support and swing up out of the way to provide a clear exit for the driver. Two universal joints connect the steering column to the Pitman triangle input shaft. This steering wheel configuration provides a natural response, similar to that of driving an automobile.

8 Chassis

The main goal for the chassis is to provide a rigid structural on which to mount the suspension, roll bar, and rear wheel brackets. The chassis must: *a*) span a wheelbase of 66 in, *b*) be as light as possible, and *c*) provide positive drainage of any fluids. The chassis is being made of AIREX C71 structural foam wrapped in a triaxial carbon fiber reinforcement.

The previous chassis design consisted of a polypropylene honeycomb core surrounded by carbon fiber-epoxy composite. This year the chassis will resemble a rail design, as seen in Fig. 11, rather than a full-width panel. The chassis design has been changed to rails because it will greatly reduce the amount of core material required and will increase rigidity since the rail has a larger moment of inertia than the previous panel design. Due to the complexity of the rail chassis design, the entire chassis will be machined from a single piece of core material. This will eliminate any joint weaknesses and the chassis dimensions will be more accurate. To provide positive drainage of the engine compartment, a sloped hole will be drilled through the completed chassis at the rear of the well in the chassis near the rear wheel. A an aluminum tube will be epoxied in place and sealed, allowing any fluids to drain out of the chassis away from the driver and exit the body through the rear wheel opening.

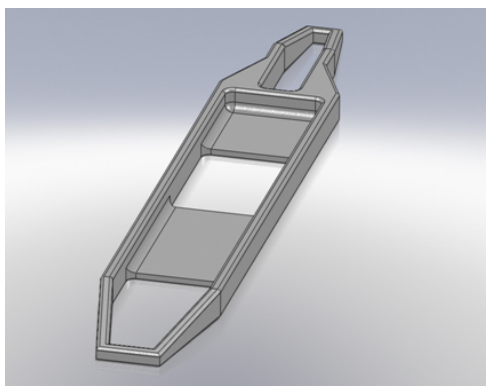

Figure 11: Rail Chassis Design

8.1 Core Material Selection

Preliminary testing was done to narrow the selection of core materials. Table 1 shows the data collected from the testing. A three point bend test was conducted on specimens that were similar to the rail in shape and dimension.

Table 1: Chassis Core Material Testing Results

Sample	Load	Strength to Weight Ratio
C71.75 Rigid	210 lb	42
C70.130 Rigid	300 lb	37
SB. 100 GP AL 600/10	280 lb	29
R63.80 Rigid	210 lb	37.5

8.2 Carbon Fiber Analysis

A Finite Element Analysis (FEA) model of the chassis was created and evaluated using MSC PATRAN to determine the required number of reinforcement layers for the chassis. For analysis purposes, the foam core is considered to have isotropic properties but differing strength in compression and tension. On the other hand, the carbon fiber-vinylester is assumed to be a linear material with orthotropic properties. The properties of the foam are taken from the company website specifications sheet[1] while the carbon fiber-vinylester resin was tested in both tensile loading and Iosipescu shear loading. The analysis results showed that two layers of carbon fiber along the longitudinal axis of the vehicle yield a safety factor of 2.1 for a loading of 1000 lb of the related wheel structure. Since composites are never perfect and may not have the same properties as the tested specimens, the chassis will use three layers of carbon fiber – vinylester resin.

8.3 Roll Bar

To ensure driver safety in the case of flipping over, a roll bar was created out of one inch 6061-T6 aluminum tubing with a thickness of 1/16 in. The roll bar was designed to hold the weight of the car and driver, with a minimum factor of safety of 1.88, determined using a 250lb. static load in SolidWorks Simulation. The final roll bar design is shown in Fig. 12. Further analysis of the roll bar in SolidWorks yielded a maximum resultant deformation of 0.0434 in, located at the point of direct load transfer. The maximum stress, according to the Von Mises Effective Stress theory, was 21.3 ksi, at the location shown in Fig. 13.

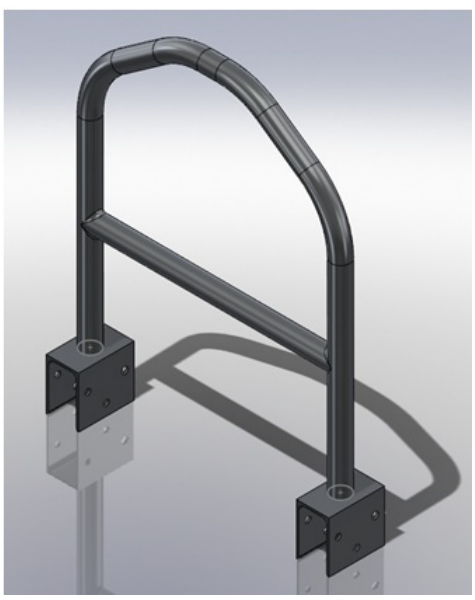

Figure 12: Roll Bar Design with C-Channels

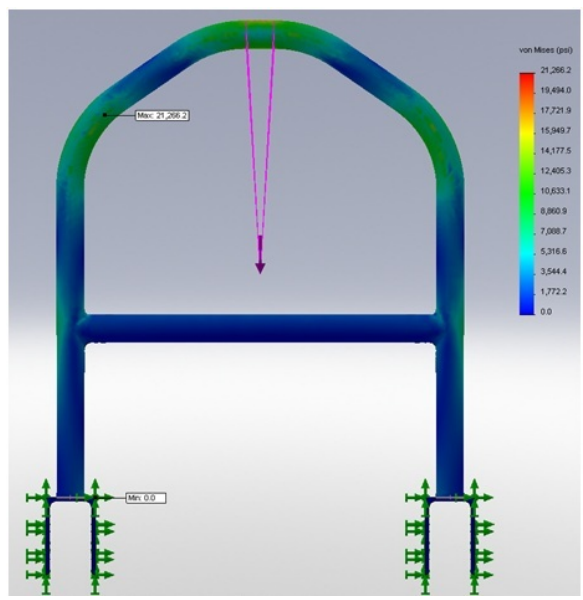

Figure 13: SolidWorks Analysis of the Roll Bar

8.4 Rear Wheel Bracket

The main design considerations for the rear wheel bracket are strength and weight. The mounting should be as light as possible while still strong enough to support the weight of vehicle over the rear wheel and the transmission of torque through the chain drive.

The material chosen for the bracket was 6061-T6 aluminum. When choosing the material, weight, strength, and the ease of use were considered. 6061-T6 is a strong enough aluminum to support all the applied forces. The other factor considered was weldability—the weld between the upright portion and the c-channel could not compromise the strength of the part. The c-channel provides a convenient, stable mounting to the chassis frame rails.

Stress analysis was performed on the rear wheel bracket using SolidWorks Simulation. The limiting load case was the vertical load as the axle would push against the bracket as seen in Fig. 14. This analysis showed that material could be removed, but also showed where material was necessary and what thickness of material was necessary. Since weight is an important factor and the part consisted of

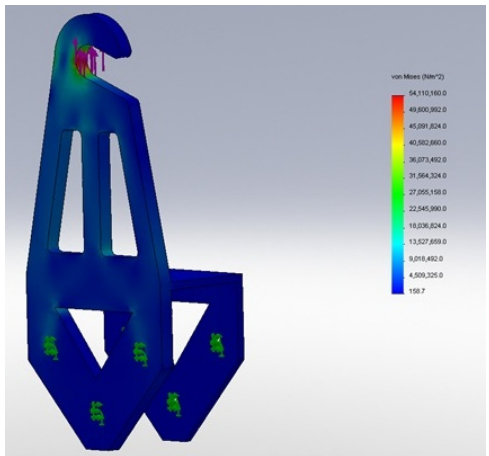

Figure 14: SolidWorks Analysis of Rear Wheel Bracket

numerous flat solid sections, material was removed while retaining the strength of the part. Material was removed in the low-stress areas in the interior of the part and around the bolt holes.

The part has many holes and sections removed which would have made machining by hand difficult and time consuming, so the parts were cut on a CNC Waterjet by sponsor TAK Engineering, Inc. This allowed for accurate cuts easily done by machine.

The bracket simply needed three bolts put through it and the rail to be firmly attached. The bolt diameter of 5/16″ was chosen to be consistent with the bolt diameters used elsewhere on the vehicle. Due to the close proximity to the wheel, sprocket, and chain, carriage bolts were used on the inner side of the rail because their low profile would prevent contact with any moving parts.

9 Body/Aerodynamic Shell

The purpose of the body is to protect the driver from outside influences such as pavement, other cars, and the elements. Another purpose is to improve the aerodynamics of the SMV. Several goals and requirements for the design process were defined.

Goals:
- Improve driver safety
- Minimize aerodynamic drag
- Minimize total surface area of body shell

Design Requirements:
- Accommodate brake light with SAE J586 standard
- Allow room for multiple team members to fit as drivers in a reclined position
- Provide space for engine and drive train components to operate safely
- Accommodate inboard wheels, including full range of movement
- Allow comfortable access to steering controls
- Offer a minimum 1 in of clearance around all components to account for future design changes
- Maintain 3 in ground clearance to prevent scraping
- Provide horizontal parting line for manufacturing

Several overall body shell concepts were created and are shown below. Before a design was selected and perfected, the overall advantages and drawbacks of each design were assessed.

9.1 Design Development

The following initial concepts, Figs. 15-17, were proposed.

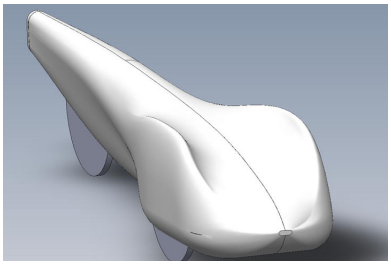

Figure 15: Body Concept 1

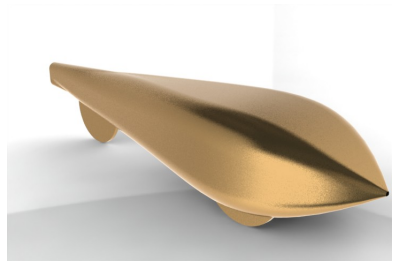

Figure 16: Body Concept 2

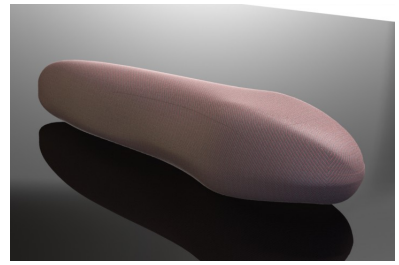

Figure 17: Body Concept 3

A decision matrix (Table 2) was generated, ranking each concept in several categories. From this decision matrix, Design 3 was selected as the starting point for the body shell. The following aerodynamic drag relationship (Eq. 7) was used to model the drag force on the vehicle.

Table 2: Decision Matrix for Body Concepts

	Frontal Surface Area	Overall Surface Area	Full Steering Range	Ease of Manufacture	Driver Comfort	Aesthetics	Totals
Design 1	2	3	1	1	1	2	13
Design 2	1	2	2	1	1	2	12
Design 3	3	1	3	3	3	2	18

Legend: 1-Poor, 2-Average, 3-Best

$$F_{drag} = \frac{1}{2} c_d \rho A V^2 \tag{7}$$

where c_d is the drag coefficient, ρ is the air density, A is the frontal area of the body, and V is the vehicle speed relative to the air. Note that both the drag coefficient and the frontal area impact the drag force linearly. Therefore, the frontal area was first reduced to a minimum, followed by curving the overall body shape to improve the coefficient of drag. The body design was analyzed using the commercial computational fluid dynamics (CFD) package StarCCM+ by CD-adapco to find ways of improving the shape of the body aerodynamically.

The model of the vehicle was simplified in the simulation by neglecting the effect of the wheels and their rotation. The body of the vehicle was placed into a box with 4 times the width of the vehicle, 5 times the height of the vehicle, and 2.5 times the length of the vehicle. This control volume, shown in Fig. 18, was selected to ensure minimal boundary interactions.

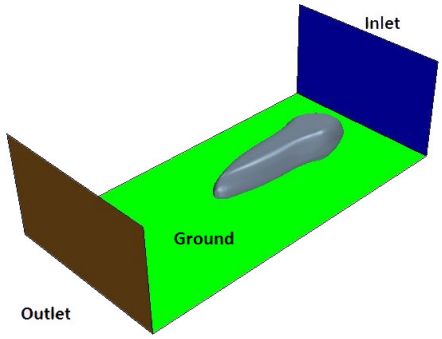

Figure 18: CFD Analysis Control Volume

The body shell was simulated in a worst case scenario, traveling at 30 mph with a 30 mph headwind through air at 23°C. The air is assumed to be an ideal gas and incompressible with turbulence. A k-ϵ turbulence model was used since it is robust and effective for parametric studies. To improve the shape, an iterative process was followed. Areas of large pressure gradient were slowly decreased. Another important variable in optimizing the body is the generated downforce. The body must not generate any lift, but it should produce as little downforce as possible.

The grid density was raised and the boundary prism layer thicknesses were decreased until the simulation was grid independent. A simulation of the final design iteration yielded a drag coefficient value of 0.11. The final body design is shown in Fig. 19.

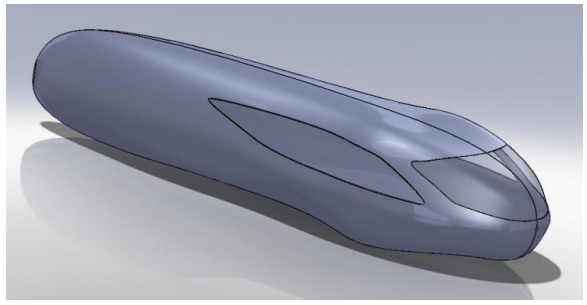

Figure 19: Final Body Design

9.2 Accessibility

For both the ease of the driver and maintenance of the vehicle, a driver hatch and rear engine hatch will be made. The hatches will be held down by magnets and have tabs as necessary to open from the outside. The body will be manufactured in two halves which will be semi-permanently attached to each other. Enough access will be provided by the hatches for normal use, but the halves can be separated and removed for major vehicle maintenance.

9.3 Construction Materials

The vehicle shell will be made using biaxial weave 5.7 oz carbon fiber with a vinylester resin. The 5.7 oz carbon fiber was chosen for its shape forming properties and the appropriate thickness for durability and resin holding weight. The vinylester resin was chosen since it produces a composite which can remain rigid at temperatures of up to 300°F, even when room temperature cured. The heat caused softenening of the epoxy resins used in the body and chassis last year, causing unwanted twisting near the motor mount. Two layers of carbon fiber/vinylester resin were chosen for minimum weight and a smooth outer surface in addition to being reinforced by a carbon wrapped foam skeleton for support. Initial testing has shown that this internal structure increases the stiffness of the body panels by a factor of four.

10 Electrical System

One of the main areas of focus on the 2010-2011 MSOE SuperMileage Vehicle is the electrical system. There are two main sections within the electrical system: the main power management system and the data acquisition/vehicle monitoring system. The first step in designing the electrical system was to analyze last year's system to determine what worked well and what could be improved.

10.1 Existing Design

For last year's competition, the power management system was basic and there was no data acquisition system. The rules were met and the vehicle passed the electrical portion of the technical inspection, but the system was far from optimized. Power management was done by using three DPDT switches wired so that if all three were in the 'on' position, 12 V from the electronic fuel injection (EFI) battery

was connected to the EFI system through the fuse box. If any of the three switches were switched off, the circuit connecting the EFI system was broken, and the kill wire on the engine was grounded, preventing the spark plug from sparking.

Analysis of this system raised a few concerns. First of all, by routing the current-carrying wires through the whole vehicle, a significant amount of the already low available power is dissipated as heat, and the voltage supplied to the EFI system is reduced. Secondly, in the event of a catastrophic failure, 12 V at potentially very high current from the battery was being routed near the driver. Finally, this configuration required low-gauge wire, which is not only harder to bend and work with, but also contributes a significant amount of weight to the vehicle.

Since there was no data acquisition system last year, the only analysis that could be done was in the form of what the team wished to be able to do. Through communication with the engine team, it was decided that a way to wirelessly monitor fuel consumption and wirelessly program the EFI system would be optimal, to allow for dynamic tuning of the engine, as well as the ability to test driving strategies for optimal fuel economy. Several other desired features were proposed for ease of use of the system, such as the ability to monitor battery levels and vehicle speed.

10.2 Power Management System

After the analysis of last year's shortcomings, the first part of designing the power management system was to see how much power was actually being lost due to the long run of the main current-carrying wires. Last year, 18-gauge wire was used, and peak load was said to be 2 A through a 25 ft wire run. The resistivity of copper wire is 0.00639 Ω/ft [4]. At 25 ft, the total wire resistance is:

$$R = \sigma\ell = \left(0.00639\frac{\Omega}{\text{ft}}\right)(25\text{ ft}) = 0.160\Omega \tag{8}$$

Using this resistance, the voltage drop across the wire given a 2 A load can be calculated as follows:

$$V = IR = (2\text{ A})(0.160\Omega) = 0.32\text{ V} \tag{9}$$

Finally, the power loss across the wire can be calculated as follows:

$$P = I^2R = (2\text{ A})^2(0.160\Omega) = 0.64\text{ W} \tag{10}$$

By speaking with the manufacturer of the EFI system, it was determined that the voltage being delivered to the EFI system has a direct correlation to its performance, so voltage drop through the wires must be eliminated as much as possible. To meet the other criteria of lighter, easier to route wires, it was desired to use much higher gauge wire. Assuming 24-gauge wire was picked, calculations 8 and 9 can be repeated to see how much power is lost due to the wire:

$$R = \sigma\ell = \left(0.02567\frac{\Omega}{\text{ft}}\right)(25\text{ ft}) = 0.642\Omega \tag{11}$$

$$V = IR = (2\text{ A})(0.642\Omega) = 1.284\text{ V} \tag{12}$$

As shown in calculation 12, the voltage drop now becomes extremely significant with a 12 V system, and this gauge of wire cannot be reliably used.

To address all of the concerns proposed above, a microcontroller-based system was chosen as the solution. By using a microcontroller to control power management on the vehicle, it is possible to control the power with logic-level voltages to provide the greatest assurance of safety to the driver. The use of logic-level control also practically eliminates wire gauge requirements as well as power loss through the wires. To control the EFI system as well as engine starting and stopping, the microcontroller will drive relays located within the fuse box. For maximum power savings and driver convenience, starting and stopping of the engine is controlled by a single button.

If all three kill switches are in the upward position, the system will allow the EFI to run and the engine to start. If any of the three switches are in the downward position, the microcontroller will cut off

power to the engine by closing a relay that grounds the spark plug and cuts off power to the EFI system by releasing a relay powering the EFI system. As a failsafe, the second set of contacts in the switches will be directly connected across the terminals of the kill relay. This guarantees that in the event of a wire or software failure, the engine will still stop when a kill switch is flipped. A pushbutton allows the driver to start the engine. If the button is pressed and quickly released, it will activate the EFI relay, allowing the fuel system to run but not start the engine. If the driver does not release the button and instead continues to hold it for a software-programmable time, the system will activate the starter relay, which activates the starter solenoid and starts the engine. This will remain until the button is released. Once the EFI system is activated, a quick press and release of the same button will turn off power to the EFI and briefly ground the spark plug. If the system is active and the button is instead held for a brief delay, the starter will be engaged again. This allows the engine to start in the event that it did not start the first time, or the user chose not to start it at first.

For this application, a very basic microcontroller is needed, as it simply needs to perform logic and basic timing operations. The requirements are that it must *a*) be easily programmable should code changes need to be made, *b*) be a through-hole part for ease of integration, *c*) be programmable in the C language for familiarity, and *d*) not require an external oscillator. After researching various 8-bit microcontrollers, the PIC16F88 from Microchip was chosen. Some features of this chip include low cost, a built in 8MHz RC oscillator, an abundance of hobbyist support, and a freely-available IDE and C compiler/assembler [7]. Thanks to the hobbyist support for this chip as well as the design of the chip in which the software has read/write access to the program memory, bootloaders are available for this chip to simplify code flashing. By utilizing the Tiny PIC Bootloader, an open source bootloader for the PIC16F88, code can be re-downloaded on the fly by simply resetting the microcontroller and downloading an updated HEX file to the device using a simple UART connection [3]. This way, code changes can be made directly in circuit without the need for special, potentially costly in-circuit programming hardware.

Thanks to a sponsor, Milwaukee Electric Tool, the vehicle's electrical system will be powered by lightweight lithium-ion batteries that can be removed and recharged at any time using a standard Milwaukee Electric Tool charger. The specific battery being used for the EFI system is the M12 48-11-2401, a 12 V battery C20 rated at 1.4 Ah. This battery meets the requirement of no larger than a 1.4 Ah EFI battery, while being simple to recharge and lightweight at 0.4 lb. For the electric starter, the Milwaukee M12 48-11-2402 battery was chosen. This battery is a 0.9 lb 12 V pack rated at 2.8 Ah, which should allow for considerable weight savings while maintaining the ability to provide plenty of starts between charges [5].

A key design feature on last year's vehicle was the use of ABS plastic enclosures for all of the electrical connections. This kept the bare connections isolated from the users while protecting the electronics from the elements and keeping the wires neat and organized. As a result, the same enclosure, a RadioShack model 270-1809, was chosen. The batteries will securely mount directly to the exterior of the enclosure using battery sockets from 12 V Milwaukee tools, and the enclosure will house all fuses, relays, and the microcontroller. Externally, binding posts will be used to connect the EFI system, data acquisition system, switches, and the connections to the starter solenoid and engine kill switch. An overall drawing of the initial layout design of the power management system is shown in Fig. 20.

10.3 Data Acquisition System

One of the biggest challenges with last year's vehicle was tuning the engine for optimal fuel economy. This is mainly attributed to the lack of a dynamometer last year, but even if a dynamometer had been available, there was no good way of monitoring the effect that small changes to the EFI system had on the overall efficiency of the engine. Since the engine consumes so little fuel, measuring how much fuel was available before and after a run is not an effective way to test the results of small changes to the EFI system. Instead, a real-time fuel consumption feedback system that could give immediate feedback to how much fuel is being consumed was needed.

Taking advantage of the EFI system, it was decided to monitor the pulse widths controlling the injector, then use that to obtain an estimate of how much fuel is being injected into the engine. On the dynamometer, this method allows the EFI system to be tuned using real-time feedback of how much fuel is being injected for a given time. On the vehicle, this same data combined with distance sensors

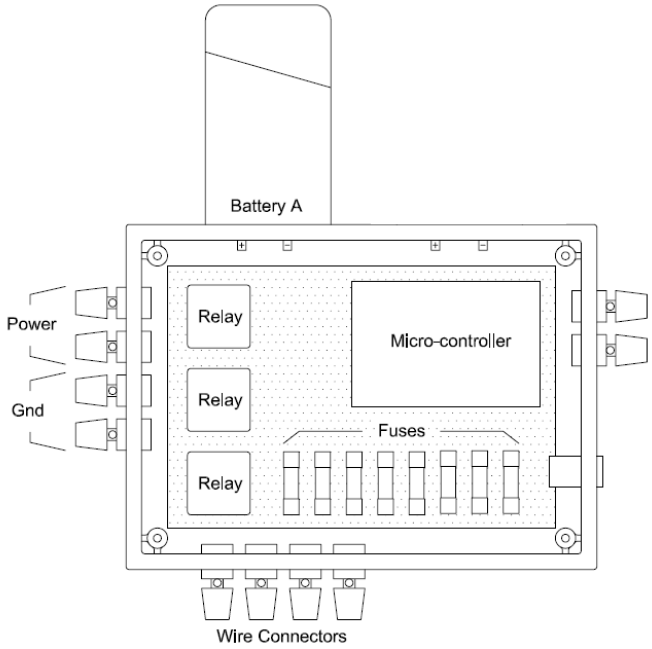

Figure 20: Initial Design of Power Management System

on the wheels can be used to determine velocity and fuel consumption per unit distance traveled.

Control Systems, Inc. (CSI), the company sponsoring the EFI system on the MSOE SuperMileage Vehicle, was initially contacted for some information on this topic. Fortunately, they had already created an injector profile relating injection volume to pulse width for a larger version of the injector on the MSOE vehicle, and knew exactly how the two injectors compared to each other. One major concern in the beginning was nonlinearity due to injector turn on/off delays. However, the experimental injector data from CSI showed that for the injection durations used by their EFI systems, turn-on/turn-off nonlinearity was negligible and the injection volume for a given pulse width could be assumed to be a linear function given the level of precision needed for this application. It was also discovered that the EFI system voltage has a significant effect on the fuel/pulse-width relationship, so the ability to monitor the EFI battery voltage and manipulate the measured data based on that voltage is critical to ensure accuracy of the measurements.

The data from the injector profile provided by CSI was modified for the injector size and then plotted as injection volume in microliters vs. pulse width in microseconds. Using those data, a linear regression equation was derived. This allows the pulse width measured by the microcontroller to be converted directly into injected fuel volume. These data are shown in Fig. 21.

To provide real-time fuel consumption data, a microcontroller-based system is needed that is capable of measuring pulse widths, performing basic mathematical operations, reading analog voltages and communicating with a PC. It is also desired to have several spare general I/O pins in case additional devices or signals are added to the system. As with the power management system, an easy-to-flash controller that is a through-hole part is essential for programming simplicity and hardware reliability. Unlike the power management system, this microcontroller has a much more challenging task to complete than simply driving relays and LEDs, meaning that the speed and performance of the microcontroller is now a concern.

Two microcontrollers were considered for this application: the same Microchip PIC16F88 chip as used in the power management system, and the ST Microelectronics STM32F100RB (shortened to STM32 from now on). On the surface, the STM32 clearly has the advantage. It is an ARM Cortex-M3-based 32-bit microcontroller, which provides a simple RISC architecture with 32-bit power [10]. It is available as part of the STM32VLDISCOVERY kit from ST Microelectronics, which is an entire development board with a USB programmer and all I/O pins accessible with standard 0.1 in pitch available for

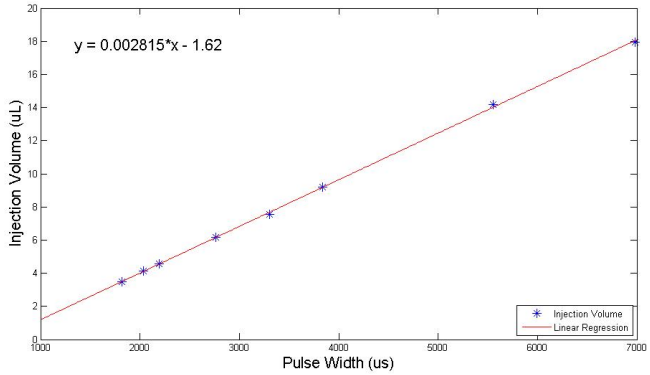

Figure 21: Injector Performance Characteristics

under $10 [11]. The core runs at up to 24 MHz and is certainly fast enough for this application. However, there are two fairly serious negative consequences to choosing this microcontroller. This microcontroller was just released on 9/14/2010, meaning that there is no hobbyist support and a lack of mature development tools[9]. Secondly, the switch to a 32-bit microcontroller from the familiar 8-bit controller is a large undertaking in itself, regardless of the RISC architecture used by the ARM core, and it would be hard to guarantee success.

On the other hand, the PIC16F88 is a familiar controller for the electrical team, and while considerably slower than the STM32, still provides all of the benefits summarized in the previous section. The 8MHz internal oscillator, while not perfect, is plenty accurate for this application, and switching to a crystal is as simple as adding the crystal and making some minor code modifications. The only unknown at this point is the ability of the microcontroller to handle 16 or 32-bit floating point operations within the required execution time.

After considering the pros and cons of both controllers, the PIC16F88 was selected, as the team is not prepared to learn an entirely new architecture without a guarantee of success. It was also decided that for this application, the loss of precision by using integers rather than floating points was a tolerable consequence for the near guarantee of success with the microcontroller.

Once a microcontroller was selected, the focus was shifted to how it will communicate with a PC. UART was chosen as the protocol due to its simplicity and widespread support between microcontrollers and PCs. However, a standard wired connection using RS232 is not an acceptable solution for the system mounted on the vehicle as it requires a wire connecting a laptop to the microcontroller mounted on the vehicle. Thus, a method of communicating wirelessly is needed. Modules called XBee, produced by Digi International, were found as a potential solution to the communications issue. These modules are based upon the ZigBee protocol, which allows for local networks to be created over basic RF technology, and are designed to be a drop-in wireless UART bridge. By simply programming the modules to communicate with each other and connecting them into the circuit, it is possible to establish a point-to-point wireless network with a maximum range of 15 miles between the microcontroller and PC [6].

With the final decisions made regarding the interface between the microcontroller, the rest of the components, and the PC, a schematic was drawn for the prototype and it was assembled. The prototype hardware was designed with the final application of mounting on the vehicle in mind. To simplify the transition from prototype to final hardware, the circuit was built exactly as the final version would be, with exception of the serial interface. Rather than attempting to get wireless working at the same time as the overall system, the prototype hardware communicates with a PC using a hard-wired RS232 connection through a MAX232 level shifter. This way, the microcontroller system can be developed and tuned without the added variable of wireless communication, and once the software and hardware is complete, the transition to wireless is as simple as replacing the MAX232 with the XBee module. The schematic is shown in Fig. 22.

Finally, the data has to be handled once it is delivered to the PC. For this task, Microsoft Visual C#

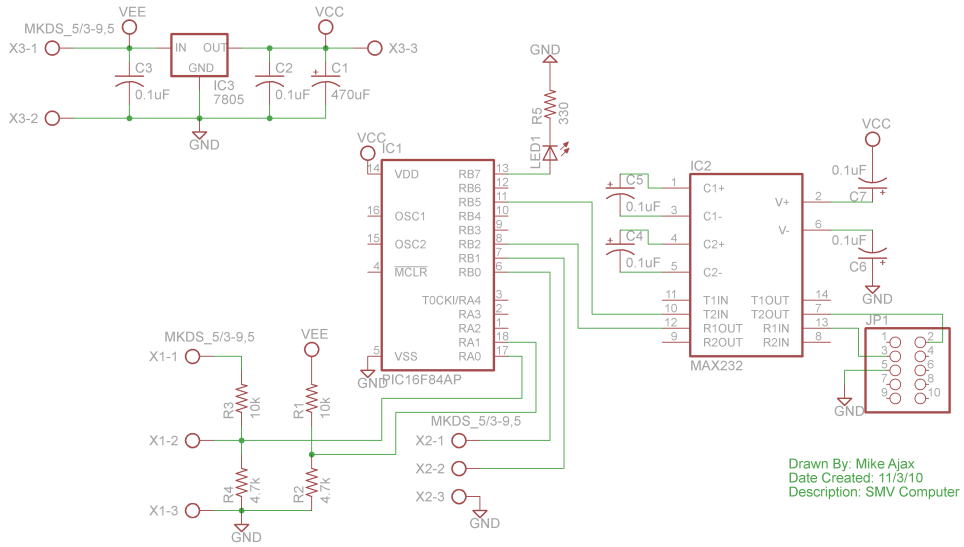

Figure 22: Data Acquisition System Schematic

.NET was chosen as the programming language. The Microsoft .NET Framework includes a library of components that make serial communications, data logging and data graphing extremely simple. The Visual C# language provides a language that strongly resembles embedded C that the electrical team members are already familiar with. Microsoft Visual Studio 2010 was chosen as the IDE since it is a top-of-the-line IDE and the Professional version is available to students at no cost through Microsoft's MSDN program. Using Visual C#, an application can be created to read the data supplied by the microcontroller, log it to a database, and perform calculations to display real-time fuel consumption, velocity, battery levels, and anything else of importance to the engine team. An alternative version of the application can also be created specifically for the dynamometer system that displays the amount of fuel injected for a given amount of time. This gives its users immediate feedback on the effects of their tuning. A screenshot of the current interface for the dynamometer application is shown in Fig. 23.

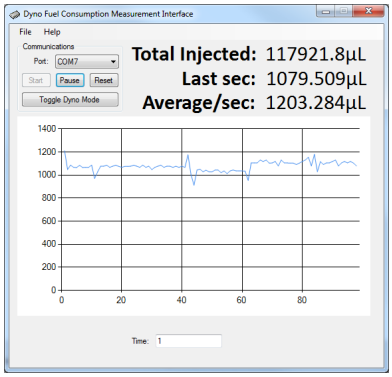

Figure 23: Dynamometer Interface Screenshot

11 Vehicle Performance

To greatly improve fuel economy, the driver uses a coast/burn strategy during the dynamic event. This strategy can provide the best efficiency while upholding the average speed requirements of the competition. The Eaton Proving Grounds track features several elevation changes. These hills allow the coast/burn strategy to be optimized, placing burns at points where they will most help the vehicle's forward motion and coasting at most other times. A Simulink model of the forces on the SMV throughout the course of a lap was generated, shown in Fig. 24. This model includes rolling resistance, aerodynamic drag, and the force of gravity on an incline. Sample calculations for these

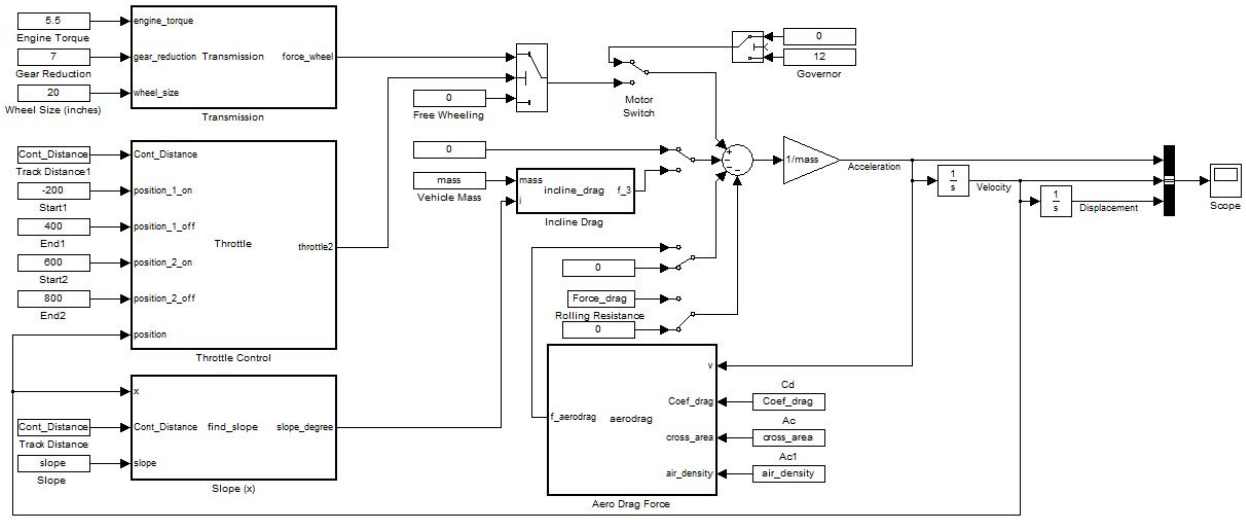

Figure 24: Simulink Block Diagram for Vehicle Simulation

forces can be found in Appendix B. The angle of inclination was determined by performing a spline fitting procedure on the provided Eaton Proving Grounds track topological data.

The top speed of the vehicle is related to the selected gear ratio and redline rpm of the engine, as in Eq. 1. The top speed of the 2011 MSOE SMV is $\boxed{38 \text{ mph}}$.

In addition to the driving strategy optimization, the modified engine will consume much less fuel than last year's stock model equipped with EFI. Initial dynamometer test data report that at a typical driving load of 3.23 ft-lbf (see Appendix B), the modified engine is nearly 25% more fuel efficient than last year's setup.

Based on the optimized driving strategy, chassis weight reduction, body enhancements, and engine improvements discussed in Section 4, the team expects to gain over 30% in fuel mileage as compared to the 2009-2010 MSOE SMV mileage of 757 mpg. A fuel mileage of $\boxed{1000 \text{ mpg}}$ is predicted for the 2011 SAE SuperMileage Competition in Marshall, MI.

12 Cost Estimate and Manufacturing Methods

The detailed cost estimates for the 2011 MSOE SuperMileage Vehicle can be found in Tables 4–8 of Appendix A. The costs for each system are summarized in Table 3. For the estimated cost, the person-hour labor estimates listed in Tables 4–8 are all billed at $10 per hour, except for items where the labor was included in the component's price (for example, the MDF Body Patterns). Throughout the vehicle

Table 3: 2011 MSOE SuperMileage Estimated Costs

Subsystem	Cost (USD)
Body	22637.70
Chassis	1503.13
Electrical	481.91
Powertrain	1791.67
Suspension	1456.84
GRAND TOTAL	27871.25

build, many different manufacturing processes were used. Most of these catered to facilities available at MSOE, such as machining, turning, CNC milling, and welding. Several specialty components were

manufactured on a waterjet owned by sponsor TAK Engineering, Inc. Also manufactured off site were the large patterns for the body, at Midwest Composite Technologies.

13 Driver Safety Features

Throughout the design process, driver safety and comfort were both top concerns. The team incorporated several features in order to satisfy the safety requirements and protect the driver. Working within the tight parameters defined by the small size of the vehicle, these important features fulfill the team's commitment to providing a safe and comfortable driving experience for all those involved.

13.1 Guards/Body

All moving components of the powertrain are shielded using carbon fiber guards to prevent damage to any electrical or fuel carrying components. Additionally, guards and sealed boxes are used to protect wires, fuel system components, and switches as well as any other electronic components. This provides another layer of safety in addition to the insulation already found on the wires. The vehicle chassis, which consists of two frame rails, is constructed with a rigid foam core sandwiched between two layers of carbon fiber. This sandwich structure serves to support the driver and can effectively distribute the applied forces, maintaining rigidity and protecting the driver in the event of a collision. The body, also constructed of carbon fiber, completely surrounds and protects the driver and critical components from outside disturbances. In all these applications, carbon fiber was selected as the material of choice for its light weight and high strength. The windshield uses an impact-resistant plastic similar to that found in safety glasses. This selection ensures the windshield will provide high visibility and will not shatter.

13.2 Roll Bar

The roll bar is made using aluminum tubing, which will provide ample strength to protect the driver in the event of a roll. This roll bar is compliant with the 250 lb load test outlined in the 2011 SAE SuperMileage Rules. The roll bar is positioned over the firewall, providing ideal protection for the driver since the drivers head partially rests against the firewall. A five-point safety harness is used to protect the driver, with the shoulder points attached to the base of the roll bar, and the three lap points attached to the vehicle frame. The harness is equipped with a single quick release latch to allow the driver to exit quickly and easily.

13.3 Firewall

The firewall is located in the same plane as the roll bar and protects the driver from fire or mechanical failure in the rear section of the car. The firewall is constructed of 0.032" aluminum sheet and reaches past the roll bar to the outer edges of the body. Any access holes and body gaps will be less than 0.5 in diameter and protected by rubber grommets and/or thick tape.

13.4 Fire Extinguisher

A dry chemical fire extinguisher (First Alert Model FE1A10GR, Rated Class 1-A:10-B:C) with pressure gauge is mounted within the driver compartment. Tubing directs the extinguishing agent through the firewall into the engine compartment. In the case of a fire, this configuration allows quick and effective response by the driver.

13.5 Suspension

In designing the suspension assembly, the team kept driver safety in mind. The steering wheel is equipped with a quick release, allowing its easy removal so the driver can exit without being impeded. To prevent interference with the driver while exiting, all wires within the driver compartment are securely fastened with no loose wiring. To prevent accidental engagement of the throttle or brake while turning the wheel, the cables connected to the hand controls are fastened down the middle of the steering column so that the rotation of the wheel does not affect the throttle or brake. Carbon fiber guards shield the drivers legs from the linkages and tie rods. Since the two front wheels are inside

the body, clear, rigid plastic guards are used to isolate them from the rest of the driver compartment while maintaining visibility.

13.6 Mirrors/Visibility

As a result of a drive to reduce air resistance on the car's body, the two rearview mirrors are located inside the driver compartment, immediately behind the two front wheels. Despite this, the mirrors provide more than adequate rearward visibility. Forward visibility is provided by a frontal windshield with two side windows that wrap around and extend from the front wheels and terminate near the drivers head position, providing superior peripheral vision—at least 90° from the longitudinal axis of the vehicle. All windshields and windows will be treated with water beading agent and anti-fogging agent to ensure visibility in inclement weather. The front windshield is large enough that the driver can easily see objects on the ground less than 20 ft away from the vehicle. The length of the side windows also allows for the rearview mirrors to be mounted on the interior while retaining effective visibility. The planned mirror placement was evaluated on the test chassis. This evaluation showed that the driver could adjust the mirrors while seated in the driving position, and also confirmed that the rearward visibility requirements in Section B9.3.2 of the official 2011 SAE SuperMileage Rules had been met. A SAE J586-compliant brake light was donated by JW Speaker, which will warn other vehicles of braking activity.

References

[1] Baltek, Inc. Airex C70 Data Sheet. Northvale, NJ, August 2010.

[2] Yunus A. Çengel and Michael A. Boles. *Thermodynamics: An Engineering Approach*. McGraw Hill, New York, 7th edition, 2011.

[3] Claudiu Chiculita. Tiny PIC Bootloader. `http://www.etc.ugal.ro/cchiculita/software/picbootloader.htm`.

[4] Cirrus Systems Corp. Resistance of Wire. `http://www.cirris.com/testing/resistance/wire.html`.

[5] Milwaukee Electric Tool Corp. 12 Volt Battery Product Information. `http://www.milwaukeetool.com/tools/cordless-tools/batteries/batteries-12-volt`, 2011.

[6] Digi International Inc. Point-to-Multipoint RF Modules. `http://www.digi.com/products/wireless-wired-embedded-solutions/zigbee-rf-modules/point-multipoint-rfmodules/`, 2011.

[7] Microchip Technology Inc. PIC16f88 Datasheet. `http://www.microchip.com/wwwproducts/Devices.aspx?dDocName=en010243`, 2005.

[8] William F. Milliken and Douglas L. Milliken. *Race Car Vehicle Dynamics*. Society of Automotive Engineers, Inc., Warrendale, PA, 12th edition, 1995.

[9] STMicroelectronics. STM32 Discovery Kit Establishes New Industry Standard for Low-Cost Tools for 32-bit Microcontrollers. `http://www.st.com/internet/com/press_release/p3065.jsp`, 2011.

[10] STMicroelectronics. STM32F100RB Value Line 32-bit Microcontrollers. `http://www.st.com/internet/mcu/product/216844.jsp`, 2011.

[11] STMicroelectronics. STM32VLDISCOVERY Discovery Board for STM32F100 MCUs. `http://www.st.com/internet/evalboard/product/250863.jsp`, 2011.

A Detailed Expense Data

The following Tables 4–8 detail the components used on the 2011 MSOE Team Carbonair SMV and their associated costs. Please note that any person-hour labor estimates listed are billed at a standard rate of $10 per hour unless the labor charge has already been included in the part cost by the sponsor.

Table 4: Estimated Cost Body

Part No	Supplier Part No	Description	Sponsor	Labor	Labor Type	Qty		Cost	Ext. Cost
B-001	CCP KF3202L-00	Vinylester Resin	CCP	10	Hand Layup	7	gal	50.00	450.00
B-002	A&P BIMAX-L-52	5.7oz Carbon Fiber	A&P Tech.	25	Hand Layup	18	yd	32.00	826.00
B-003	Foam Rope - 20 ft	Reinforcing Core Material	Purchased	0.5	Hand Layup	3	rl	4.00	17.00
B-004	US Comp. VB-VF02110	Peel-Ply Release Fabric	Purchased	0.25	Vacuum Bagging	11	yd	5.50	63.00
B-005	ECI BR-4OZ-60IN	Breather Fabric	Purchased	0.5	Vacuum Bagging	18	yd	2.90	57.20
B-006	ECI TA-LT-60FT	Vacuum Seal Tape	Purchased	0.25	Vacuum Bagging	2	rl	7.00	16.50
B-007	ECI BF-HD-120IN	Heavy Duty Bag Film	Purchased	0.5	Vacuum Bagging	11	yd	3.90	47.90
B-008	US Comp. TR-104-HT	HT Mold Release Wax	Purchased	0.5	Fiberglass Molds	1	pc	13.95	18.95
B-009	US Comp. FG-10538	Chopped Fiberglass Mat	Purchased	4	Fiberglass Molds	50	yd	2.35	157.50
B-010	CCP 945YJ071	Gel Coat	CCP	4	Fiberglass Molds	1	gal	60.00	100.00
B-011	Exp. Comp. RL-FB-3IN	0.5x3″ Fiberglass Roller	Purchased	0	Fiberglass Molds	3	pc	6.50	19.50
B-012	Exp. Comp. RL-FB-5IN	0.5x5″ Fiberglass Roller	Purchased	0	Fiberglass Molds	3	pc	6.75	20.25
B-013	MCT-SMV-002T	Upper MDF Pattern	MCT	0	MDF Patterns	1	ct	10000.00	10000.00
B-014	MCT-SMV-002B	Lower MDF Pattern	MCT	0	MDF Patterns	1	ct	10000.00	10000.00
B-015	3M-100/250/800/2K	Sandpaper	Purchased	25	MDF Patterns	4	pk	30.00	370.00
B-016	Hawkeye 714-001	Duratec Poly. Sealer	Purchased	3	MDF Patterns	1	qt	55.00	85.00
B-017	Hawkeye 702-003	Duratec Poly. Base Primer	Purchased	3	MDF Patterns	2	gal	62.41	154.82
B-018	Hawkeye 714-003	Duratec Poly. Clear Gloss	Purchased	3	MDF Patterns	1	gal	85.46	105.46
B-019	Hawkeye 714-004	Duratec Poly. Surf. Primer	Purchased	3	MDF Patterns	1	gal	30.00	60.00
B-020	Hawkeye 714-005	Duratec Thinner	Purchased	0	MDF Patterns	1	gal	28.64	28.64
B-021	Aqua-Buff 1/2000W	Polishing Compound	Purchased	2	MDF Patterns	2	ct	10.00	40.00
								Body Subtotal:	22637.70

Table 5: Estimated Cost Chassis

Part No	Supplier Part No	Description	Sponsor	Labor	Labor Type	Qty		Cost	Ext. Cost
C-001	Airex C71.55	Core Material	3A Composites	15	CNC Machining	1	st	250.00	400.00
C-002	A&P 10.2 oz CF	Fiber Reinforcement	A&P Technologies	10	Hand Layup	1	yd	582.85	682.85
C-003	CCP Vinylester Resin	Matrix Material	Cook Composites	10	Hand Layup	3	gal	50.00	250.00
C-004	SM t61r.875x.065-60	Roll Bar Tube	Purchased	5	Bend & Weld	1	pc	11.58	61.58
C-005	SM 61a.188.3-12	Roll Bar Chassis Mount	Purchased	4	Machine & Weld	2	pc	8.50	57.00
C-006	SM t61r.875x.065-60	Rear Wheel Bracket	Purchased	3	Machine & Weld	2	pc	8.00	46.00
C-007	SM 61r.375-12	Bolt Insert	Purchased	0.5	Cut	14	pc	0.05	5.70
								Chassis Subtotal:	1503.13

Table 6: Estimated Cost Electrical

Part No	Supplier Part No	Description	Sponsor	Labor	Labor Type	Qty		Cost	Ext. Cost
E-001	RadioShack 270-1801	3″x2″x1″ Project Enclosure	Purchased	0	N/A	2	pc	2.49	4.98
E-002	RadioShack 270-1806	7″x5″x3″ Project Enclosure	Purchased	0	N/A	1	pc	5.99	5.99
E-003	RadioShack 276-170	550-Hole PCB	Purchased	0	N/A	3	pc	2.99	8.97
E-004	RadioShack 275-652	DPDT Toggle Switch	Purchased	0	N/A	3	pc	3.99	11.97
E-MISC	Assorted	Resistors, Capacitors, etc.	MSOE	0	N/A	1	asst	20.00	20.00
E-005	Microchip PIC16F88	PIC16F88 Microcontroller	Microchip	0	N/A	3	pc	4.00	12.00
E-006	MET 48-11-2402	MET M12 Ext. Cap. Battery Pack	Milw. Tool	0	N/A	1	pc	117.00	117.00
E-007	MET 48-11-2401	Milw. Tool M12 Battery Pack	Milw. Tool	0	N/A	1	pc	70.00	70.00
E-008	MET 48-59-2401	Milw. Tool M12 Battery Charger	Milw. Tool	0	N/A	1	pc	82.00	82.00
E-009	Xbee XBP09-XC009-DK	Xbee XSC Development Kit	Purchased	0	N/A	1	pc	149.00	149.00
								Electrical Subtotal:	481.91

Table 7: Estimated Cost Powertrain

Part No	Supplier Part No	Description	Sponsor	Labor	Labor Type	Qty		Cost	Ext. Cost
P-001	Horstman #219-96T	96 Tooth Sprocket	Purchased	0	N/A	1	pc	15.00	15.00
P-002	DID #219-DHA-114L	#219 Steel Chain	Purchased	0	N/A	1	pc	56.00	56.00
P-003	Horstman X5-CL-FD32	X5 Clutch Friction Disc	Purchased	0.5	Assembly	1	pc	20.57	25.57
P-004	Horstman RB-875-X5	0.875″x1.25″ Clutch Roller Bearing	Purchased	0.5	Assembly	1	pc	8.04	13.04
P-005	Horstman TB-X5	Clutch Thrust Bearing	Purchased	0	N/A	1	pc	3.06	3.06
P-006	B & S 091202 T1016	Base Engine	B & S	10	Modification	1	pc	455.00	555.00
P-007	Bosch 0280155989	Fuel Injector	Purchased	0	N/A	1	pc	40.00	40.00
P-008	CSI ECU-FCR-5	FCR-5 Engine Control Unit	CSI	8	Tuning	1	pc	599.00	679.00
P-009	KNG F30KP.27DC	Fuel Pump	Purchased	0	N/A	1	pc	110.00	110.00
P-010	Megan Racing FPR-U	Fuel Pressure Regulator	Purchased	0.5	Assembly	1	pc	60.00	65.00
P-011	Assorted	EFI Fittings / Valves	Purchased	1	Assembly	1	asst	50.00	60.00
P-012	Honda CRF-50	Cylinder Head	Purchased	3	Modification	1	pc	60.00	90.00
P-013	Wiseco XR-50 88-03 CRF-50F	Piston	Purchased	2	Prep	1	pc	60.00	80.00
								Powertrain Subtotal:	1791.67

Table 8: Estimated Cost Suspension and Running Gear

Part No	Supplier Part No	Description	Sponsor	Labor	Labor Type	Qty		Cost	Ext. Cost
S-001	SM 61a.188.3-12	Suspension Frame	Purchased	15	Machine & Weld	1	pc	84.68	234.68
S-002	SM 40b.234.5-85	Integrated Axle-Kingpin	MSOE	10	Machine & Weld	2	pc	14.56	129.12
S-003	McMaster-Carr 8554K8	MDS-Filled Nylon Bushing	Purchased	2	Machine	1	ft	8.50	28.50
S-004	SM 61a.255.3-12	Pitman Triangle	Purchased	2	CNC Machining	1	pc	10.43	30.43
S-005	SM 61a.375-18	Left Output Link	Purchased	2	CNC Machining	1	pc	16.12	36.12
S-006	SM 61a.375-18	Right Output Link	Purchased	1.5	CNC Machining	1	pc	16.12	31.12
S-007	SM 61t.156-72	Driver Controls	Purchased	4	Machine & Weld	1	pc	14.00	54.00
S-008	McMaster 60685K321/2	Tie Rod Ends	Purchased	0	N/A	4	pc	13.81	55.24
S-009	HBPSI SM714K	14G Brass Spoke Nipple	HB Performance	0	N/A	100	pc	0.65	65.00
S-010	HBPSI SB3207	207 mm DB Black Spoke	HB Performance	0	N/A	100	pc	0.65	65.00
S-011	HBPSI EHKM32016T	Abbah Front Hub 32H	HB Performance	0	N/A	2	pc	38.93	77.86
S-012	HBPSI 070E150236051	Assault SL-1 Rim 32H	HB Performance	0	N/A	2	pc	28.14	56.28
S-013	KHE HU9377	Astern Freehub LHD 36H	Purchased	0	N/A	1	pc	132.00	132.00
S-014	HBPSI 070E150259634	Rhyno Lite XL Rim 36H	HB Performance	0	N/A	1	pc	39.86	39.86
S-015	Primo B001F6ZFM6	Comet 20x1-1/8″ Front Tire	Purchased	0	N/A	2	pc	35.00	70.00
S-016	HBPSI 1428857	Hayes El Camino Disc Brake Caliper	HB Performance	2	Assembly & Bleed	2	pc	56.43	132.86
S-017	HBPSI 002SR1K16	Hayes Stroker Trail Brake Lever	HB Performance	1	Assembly & Bleed	1	pc	78.32	88.32
S-018	HBPSI 0017GMWV6	Hayes V-6 160 mm Brake Rotor	HB Performance	2	N/A	2	pc	28.74	77.48
S-019	HBPSI 001CJVC00	Hayes Bleed Kit	HB Performance	2	Assembly & Bleed	1	pc	32.97	52.97
								Suspension Subtotal:	1456.84

B Engine Displacement Calculations

The calculations below, performed to determine the smaller displacement for the engine, assume an ideal Otto Cycle. This assumption was used to simplify the analysis to obtain an educated ballpark figure for the power output from 50cc. This power output was then compared to the required power output to drive the SMV around the Eaton Proving Grounds. A displacement of 50cc was chosen for the analysis because acquiring parts, such as a head and piston, to retrofit the stock engine would be relatively simple.

The first step in determining if 50cc would produce sufficient power was to calculate the amount of power required for the vehicle to complete a lap at the Eaton Proving Grounds. The assumptions used to model the car's trip around the track were a worst case scenario, meaning the times at which the most power would be required. These assumptions included starting from 0 mph and accelerating to a speed of 30 mph at a rate of 1 mph/s while traveling up a 1° incline.

In order to determine how much force was required to overcome all the losses, including drag, rolling resistance, and gravity, Newton's 2nd Law is applied as in Eq. 13:

$$\Sigma F = ma \tag{13}$$

Applying Newton's 2nd Law to the assumed losses resulted in Eq. 14:

$$F_{\text{engine}} - F_{\text{f,drag}} - F_{\text{f,rolling}} - F_{\text{incline}} = ma \tag{14}$$

In order to determine the value of F_{engine}, the values of all the other unknowns in Eq. 14 were needed. A few key equations were used to obtain these values.

First the drag force was calculated using Eq. 7 in §9. Since the drag force is a function of velocity and thus increases as velocity increases, it was calculated for velocities between 0mph and 40mph (the approximate top speed, as computed in Eq. 1) in increments of 1 mph.

Next, the rolling resistance was calculated using Eq. 15, where C_r is the coefficient of rolling resistance, a tabulated value for the type of tires and bearings the vehicle uses.

$$F_{\text{f,rolling}} = C_r g m_{\text{SMV}} \tag{15}$$

In order to determine the force that the incline imposed on the vehicle, a simple free body diagram of the vehicle on a one degree incline was used. The force in the direction that imposes forward motion of the vehicle and therefore required more power output from the engine was calculated using Eq. 16:

$$F_{\text{incline}} = m_{\text{SMV}} g \sin 1^\circ \tag{16}$$

These force equations along with the mass of the vehicle and the desired acceleration rate were substituted into Eq. 14, then rearranged to solve for the force required from the engine. The acceleration was determined using Eq. 17:

$$a = \frac{(v_f - v_i)}{t_{\text{burn}}} \tag{17}$$

Where the initial velocity is 0 mph, the final velocity is 30 mph, and the burn time is 30 s, chosen because this was the average amount of time that the driver engaged the engine during a single burn event while on the track during the 2010 competition.

The spreadsheet used to calculate the power output required for the engine to run the vehicle at 30mph using Eqs. 14-17 is presented in Table 9.

The plot of rolling resistance, drag force, and force of the incline with respect to velocity, is presented in Fig. 25.

Table 9: Vehicle Force Calculations

Aerodynamic Drag			Rolling Resistance					
Cd=	0.1044		C_r=	0.0015				
A=	0.39547018	m^2	g=	9.81	m/s^2			
ρ=	1.142	kg/m^3	m_{SMV}=	101.15	kg			
v [mph]	v [m/s]	F_d [N]	F_r [N]	F_s [N]	F_e [N]	E_{out} [KJ]	P_{out} [kW]	P_{out} [hp]
0	0.0000	0.0000	1.4884	17.3177	64.0242	12.880		
1	0.4470	0.0047	1.4884	17.3177	64.0289	12.881		
2	0.8941	0.0188	1.4884	17.3177	64.0431	12.883		
3	1.3411	0.0424	1.4884	17.3177	64.0666	12.888		
4	1.7882	0.0754	1.4884	17.3177	64.0996	12.895		
5	2.2352	0.1178	1.4884	17.3177	64.1420	12.903		
6	2.6822	0.1696	1.4884	17.3177	64.1938	12.914		
7	3.1293	0.2309	1.4884	17.3177	64.2551	12.926		
8	3.5763	0.3015	1.4884	17.3177	64.3257	12.940		
9	4.0234	0.3816	1.4884	17.3177	64.4058	12.956		
10	4.4704	0.4711	1.4884	17.3177	64.4954	12.974		
11	4.9174	0.5701	1.4884	17.3177	64.5943	12.994		
12	5.3645	0.6784	1.4884	17.3177	64.7026	13.016		
13	5.8115	0.7962	1.4884	17.3177	64.8204	13.040		
14	6.2586	0.9234	1.4884	17.3177	64.9476	13.065		
15	6.7056	1.0600	1.4884	17.3177	65.0843	13.093		
16	7.1526	1.2061	1.4884	17.3177	65.2303	13.122		
17	7.5997	1.3616	1.4884	17.3177	65.3858	13.154		
18	8.0467	1.5265	1.4884	17.3177	65.5507	13.187		
19	8.4938	1.7008	1.4884	17.3177	65.7250	13.222		
20	8.9408	1.8845	1.4884	17.3177	65.9087	13.259		
21	9.3878	2.0777	1.4884	17.3177	66.1019	13.298		
22	9.8349	2.2803	1.4884	17.3177	66.3045	13.338		
23	10.2819	2.4923	1.4884	17.3177	66.5165	13.381		
24	10.7290	2.7137	1.4884	17.3177	66.7379	13.426		
25	11.1760	2.9446	1.4884	17.3177	66.9688	13.472		
26	11.6230	3.1849	1.4884	17.3177	67.2091	13.520		
27	12.0701	3.4346	1.4884	17.3177	67.4588	13.571		
28	12.5171	3.6937	1.4884	17.3177	67.7179	13.623		
29	12.9642	3.9622	1.4884	17.3177	67.9864	13.677		
30	13.4112	4.2402	1.4884	17.3177	68.2644	13.733	0.4578	0.6139
31	13.8582	4.5276	1.4884	17.3177	68.5518	13.790		
32	14.3053	4.8244	1.4884	17.3177	68.8486	13.850		
33	14.7523	5.1306	1.4884	17.3177	69.1549	13.912		
34	15.1994	5.4463	1.4884	17.3177	69.4705	13.975		
35	15.6464	5.7714	1.4884	17.3177	69.7956	14.041		
36	16.0934	6.1059	1.4884	17.3177	70.1301	14.108		
37	16.5405	6.4498	1.4884	17.3177	70.4740	14.177		
38	16.9875	6.8032	1.4884	17.3177	70.8274	14.248		
39	17.4346	7.1659	1.4884	17.3177	71.1901	14.321		
40	17.8816	7.5381	1.4884	17.3177	71.5623	14.396		

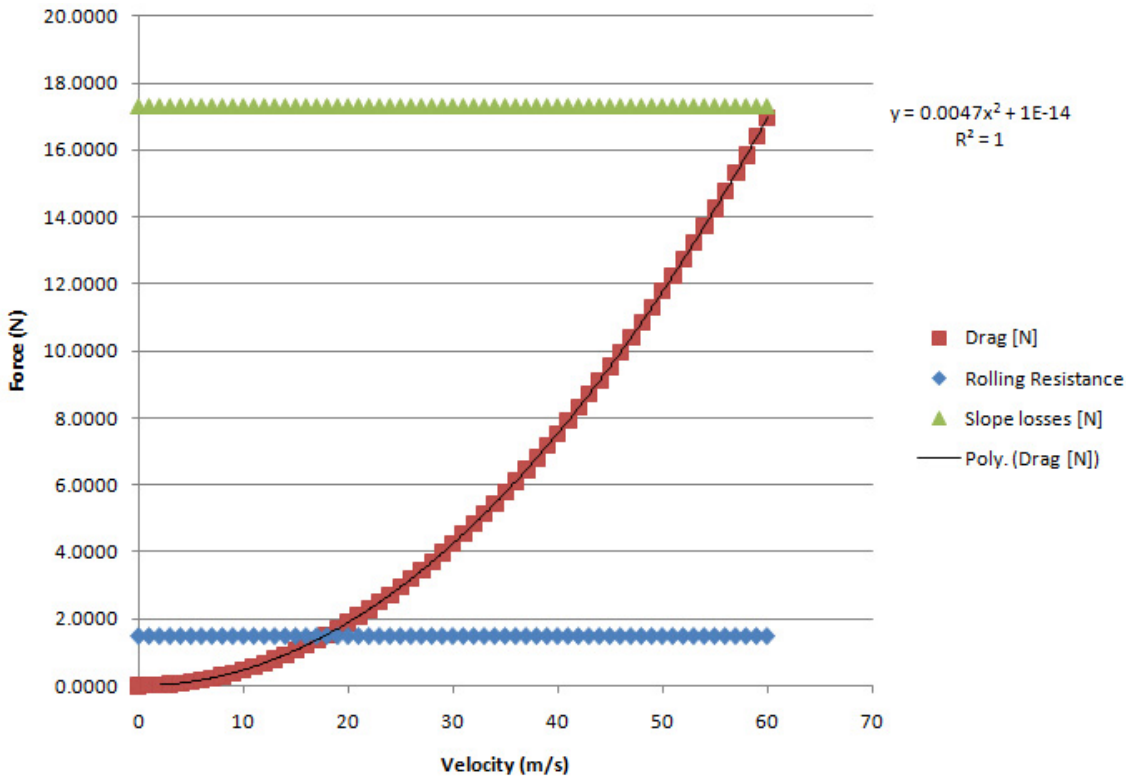

Figure 25: Comparison of Non-Conservative Forces vs. Velocity

The next step in determining if 50cc would output sufficient power was to calculate how much power could be delivered by the 50cc engine and compare to the required power of approximately 0.614 hp. As mentioned before, an ideal Otto Cycle for a 4 stroke engine was used as a model for these calculations. A plot of this cycle is shown in Fig. 26, where State 1 is when the piston is at bottom dead center (BDC), State 2 is at maximum compression (TDC), State 3 is the instant immediately after ignition, and State 4 is at BDC after the power stroke of the piston.

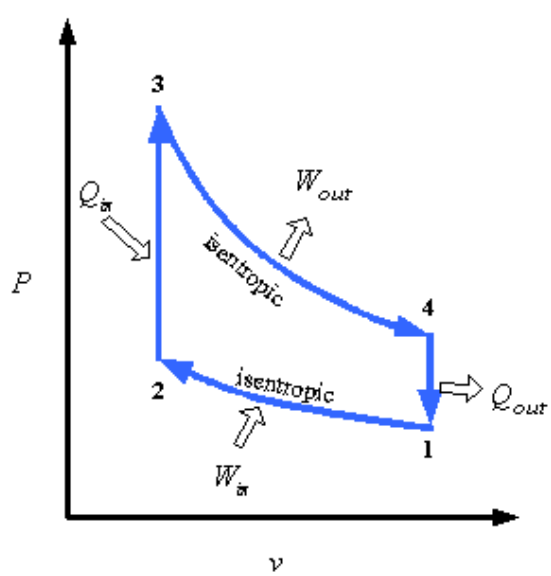

Figure 26: Otto Cycle p-v Diagram

First, State 1 was defined, as in Table 10:

Table 10: State 1 (BDC) Parameters

Temperature (T_1)	25 ˚ C = 298 K
Pressure in Cylinder (P_1)	101.26 kPa
Relative Air Pressure in Cylinder ($P_{r,1}$)	1.3068
Volume in Cylinder (V_1)	50 cm^3 = 5.0x10^-5 m^3
Relative Air Volume in Cylinder ($V_{r,1}$)	631.9
Internal Energy of the System (U_1)	212.64 kJ/kg

Where T_1, P_1, and V_1 were standard conditions and other values were found in the Thermodynamic Property Tables.[2]

Some other important values for the analysis were also defined, as listed:

- Density of Air (ρ_{air}) = 1.2 kg/m^3
- Desired Compression Ratio (CR) = 10
- Heating Value of Fuel (HV_{fuel}) = 48000 kJ/kg

In order to fix or define State 2, the following series of equations were used. The mass of air inside the cylinder as determined by Eq. 18:

$$m = \rho V = 1.20\frac{\text{kg}}{\text{m}^3}(5.0\text{x}10^{-5}\text{m}^3) = 60\text{x}10^{-6}\text{kg} \tag{18}$$

The mass of fuel as determined by the stoichiometric balance of the fuel's combustion and Eqs. 20 and 21.

$$\text{C}_8\text{H}_{18} + 12.5(\text{O}_2 + 3.76\text{N}_2) \rightarrow 8\text{CO}_2 + 9\text{H}_2\text{O} + 12.5(3.76\text{N}_2) \tag{19}$$

Air-Fuel Ratio:

$$\text{AFR} = \frac{m_{\text{air,mol}}}{m_{\text{fuel,mol}}} = \frac{(12.5)(4.76)(29\frac{\text{kg}}{\text{kmol}})}{(8-12+18)\frac{\text{kg}}{\text{kmol}}} = 15.14 \tag{20}$$

Fuel Mass:

$$m_{\text{fuel}} = \frac{m_{\text{air}}}{\text{AFR}} = \frac{60\text{x}10^{-5}\text{m}^3}{15.14} = 3.96\text{x}10^{-6}\text{kg} \tag{21}$$

Volume in Cylinder, State 2:

$$V_2 = \frac{V_1}{\text{CR}} = \frac{5\text{x}10^{-5}\text{m}^3}{10} = 5\text{x}10^{-6}\text{m}^3 \tag{22}$$

Relative Air Volume in Cylinder at State 2:

$$V_{\text{r},2} = \frac{V_2(V_{\text{r},1})}{V_1} = \frac{(5\text{x}10^{-6}\text{m}^3)(631.9)}{5\text{x}10^{-5}\text{m}^3} = 63.19 \tag{23}$$

Using the calculated properties at State 2, the following values were found using the Thermodynamic Property Tables. The temperature is 725.583 K, the relative air pressure is 33.00, the internal energy is 532.57 kJ/kg, and the in-cylinder pressure is calculated as in Eq. 24:

$$P_2 = \frac{P_{\text{r},2}(P_1)}{P_{\text{r},1}} = \frac{(33.00)(101.28\text{ kPa})}{1.3068} = 2557.1\text{ kPa} \tag{24}$$

The results of State 2 are shown in Table 11.

Table 11: State 2 (TDC) Parameters

Temperature (T_2)	725.583 K
Pressure in Cylinder (P_2)	2557.1 kPa
Relative Air Pressure in Cylinder ($P_{r,2}$)	33.00
Volume in Cylinder (V_2)	5.0x10^{-}6 m^3
Relative Air Volume in Cylinder ($V_{r,2}$)	63.19
Internal Energy of the System (U_2)	532.57 kJ/kg

A similar procedure was followed to analyze and define States 3 and 4. With the four states of the Otto Cycle defined, the net work of the engine could be determined from an analysis of the work into the system between states 1 and 2, and work out of the system between states 3 and 4.

Further analysis of the net work was done using efficiency values and the engine's indicated mean effective pressure (IMEP) value. The following Eqs. 25-26 were used. First, the ideal net work was calculated where the IMEP value was obtained from an engine comparison table.

$$W_{\text{net,ideal}} = \text{IMEP}(V_{\text{disp}}) = 1595.76 \text{ kPa}(5\text{x}10^5\text{m}^3) = 0.07979 \text{ kJ} \tag{25}$$

Next, an estimate of the actual net work was computed where the thermal efficiency of the engine was used. An ideal thermal efficiency of 47.6% was used and an actual or expected thermal efficiency of 20% was used since these are both common values for thermal efficiencies in small engines.

$$W_{\text{actual,est.}} = (W_{\text{net,ideal}})\frac{\eta_{\text{expected}}}{\eta_{\text{ideal}}} = 0.07979 \text{ kJ}\left(\frac{0.20}{0.476}\right) = 0.03352 \text{ kJ} \tag{26}$$

Finally, the estimated net work value was converted to kW and then to hp for a more practical result which is shown in Eq. 27.

$$W_{\text{net,Est.}} = 0.6705 \text{ kW} = \boxed{0.899 \text{ hp}} \tag{27}$$

Comparing this value of 0.899 hp to the amount of horsepower required, 0.614 hp, it was concluded that by sleeving the engine to 50cc the vehicle will have power to navigate the track at Eaton Proving Grounds.

C Intake Design

The intake design for the EFI system is presented in Fig. 27.

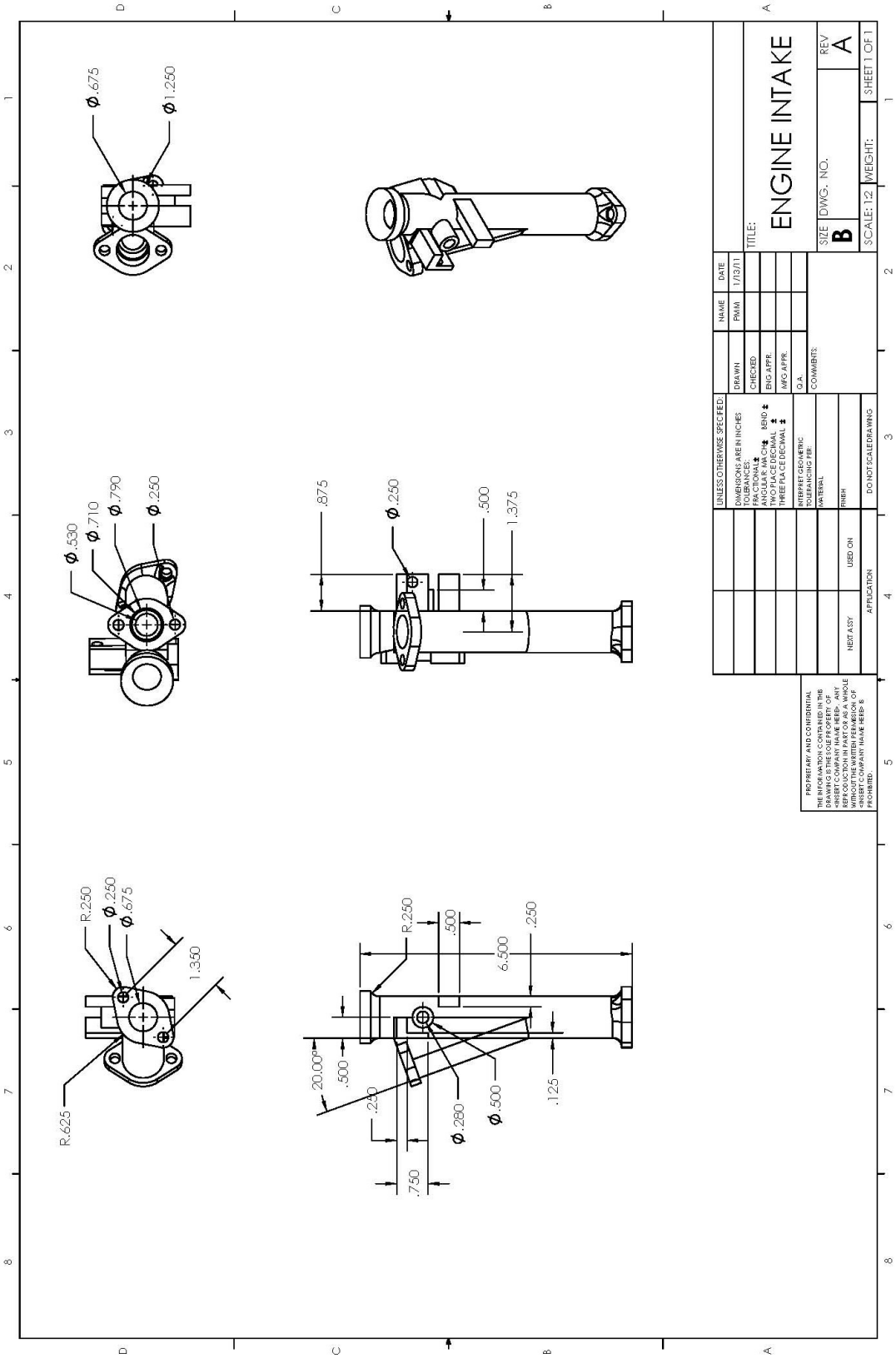

Figure 27: EFI Intake Design

D Dynamometer Tuning Equipment / Process

The purpose of the dyne testing program is to provide a way to calibrate and analyze performance of the engine. The engine utilizes alpha-n computer controlled fuel injection and ignition timing. In the alpha-n algorithm, basic fuel injection volume and spark advance values are pulled from two-dimensional look-up tables with axes alpha (throttle position) and n (engine speed). The basic values for spark advance and fuel injection volume are then multiplied by corrections from other one-dimensional look up tables for engine temperature, intake air temperature, barometric pressure and acceleration.

At its most basic level of operation, the dyne system is required to bring the engine to all of the operating conditions for steady state calibration of the fuel and spark advance maps. The hardware necessary to accomplish this task is a dynamometer to provide a load for the engine, an actuator to control the throttle, a transducer to measure torque, and a data acquisition and control system.

MSOE's existing test cell facilities provided a great starting point, complete with a cast iron test bed, exhaust fans, and wire trenches in the floor.

A 20 HP Allen Bradley electric motor and variable frequency drive were used as the dynamometer. Power absorbed by the dynamometer during testing is dissipated through a 20 HP resistive load bank. The motor drive can be operated in either a speed control mode or a torque control mode. The motor drive reports shaft torque to within $\pm$ 5%, which is adequate for this application. The throttle is actuated with a Dyne Systems DTC-1 throttle controller. Data acquisition and all necessary control is handled by a PC running LabView software.

For steady state tuning, the engine will be held at a given operating point. Initially, the air/fuel mixture is rich and the ignition timing retarded. The air/fuel mixture is then progressively leaned until lean best torque is found. Further testing and oxygen sensor feedback will serve as guides as to whether or not lean best torque is the optimum air/fuel ratio for our application. A similar process is performed to determine the optimum spark advance. The ignition timing is steadily advanced until either torque begins to fall off or detonation begins.

After steady state tuning, the flexible controls in LabView will allow simulation of the load that the engine will see in the SMV. This functionality will allow tuning for transient effects and analysis of driving style.

E Complete Team Roster

Officers:

- Chief Executive Officer: Alex Zelhofer
- Project Manager: Mike Peterson
- Media Manager: Nerissa Hanson
- Sponsorship Manager: Mike Ajax
- Treasurer: Troy Henke

Drivers:

- Troy Henke
- Meghan Krause

Body Design:

- Matt Drea
- Caleb Nitz
- Jacob Rogahn
- Charlie Scanlon
- Alex Zelhofer*†

Chassis Design:

- Troy Henke†
- Jacob London*†
- Mike Macak
- Calvin Meulemans†
- John Pondo
- Rob Runte

Dynamometer Construction:

- Patrick Comiskey
- Mike Ellingboe
- Meghan Krause
- Adam Lange*
- Michael Storm

Powertrain Design:

- Christopher Dostal
- Travis DuMez
- Nerissa Hanson†
- Eric Larson
- Eli Leggett
- Paul Marchant
- Chris Patzke
- Mike Peterson*†
- Matt Wirtz†

Electrical Design:

- Mike Ajax*†
- Dominic Frost
- Kris Kata

Steering Design:

- Todd Brooke
- Paul Gessler*†
- Scott Gray
- Marshall Schaeffer†
- Tyler Wudstrack†

* Denotes Team Leader
† Denotes Returning Member